Fall Inducing Movable Platform (FIMP) for Overground Trips and Slips

Jie Kai Er (erjiekai@gmail.com)
Nanyang Technological University https://orcid.org/0000-0001-5538-6084
Cyril John William Donnelly
Nanyang Technological University
Seng Kwee Wee
Tan Tock Seng Hospital
Wei Tech Ang
Nanyang Technological University

Research

Keywords: Balance, Overground Walking, Fall inducing platforms, Ankle perturbation, Statistical Parametric Mapping

Posted Date: January 21st, 2020

DOI: https://doi.org/10.21203/rs.2.21449/v1

Version of Record: A version of this preprint was published at Journal of NeuroEngineering and Rehabilitation on December 1st, 2020. See the published version at https://doi.org/10.1186/s12984-020-00785-0.

RESEARCH

Fall Inducing Movable Platform (FIMP) for Overground Trips and Slips

Jie Kai Er[1*], Cyril J Donnelly[1], Seng Kwee Wee[2] and Wei Tech Ang[1]

Abstract

Background: The study of falls and any related fall prevention/intervention device requires the recording of true falls incidence. However, true falls are rare, random and difficult to collect. Therefore, a system that can perturb falls in an ecologically valid and repeatedly manner will greatly benefit the understanding of the neuromuscular mechanisms underpinning real-world falls events.

Methods: A fall inducing movable platform (FIMP) was designed to arrest and accelerate the subject's ankle to induce trip via a brake and slip via a motor respectively. A gait phase detection algorithm was also created to allow the timely activation of the fall mechanisms to induce different recovery actions. Statistical Parametric Mapping (SPM1D) and two sample t-test were used to evaluate the transparency of the platform before it was used to induce falls. Thereafter, SPM1D and one-way repeated measure ANOVA were used assess the effectiveness of FIMP in inducing realistic falls.

Results: Walking with the FIMP's fall mechanisms attached on the ankle (SW) was found to be similar to normal walking (NW), except for a slight increase in ankle flexion during the swing phase. However, the magnitude of change would be considered negligible when compared to the changes in joint angles during the trips and slips of interest.

During the FIMP induced trips, the brake activates at the terminal-swing and mid-swing gait phase to induce the lowering and skipping strategies respectively. The characteristic leg lowering and the subsequent contralateral leg swing was seen in all subjects for the lowering strategy. Likewise, for skipping strategy, all subjects skipped forward on the perturbed leg. On the other hand, slip was induced by FIMP using the motor to impart unwanted forward acceleration to the ankle with the help of friction-reducing ground sliding sheets. Joints stiffening was observed during slips, and subjects adopt the *surfing* strategy after the initial slip.

Conclusion: Results indicate that FIMP can induce reliable and ecologically valid falls repeatedly under simulated experimental conditions. The usage of SPM1D with FIMP allows the creation of the first ever quantifiable trip and slip reactive kinematics comparison. Effects of fall recovery anomalies can now be easily identified.

Keywords: Balance; Overground Walking; Fall inducing platforms; Ankle perturbation; Statistical Parametric Mapping

Background

On average, elderly population(s) (age≥65) encounter falls incidence at a weighted mean rate of 0.65 times annually, and this rate doubles for individuals above 75 years old [1]. The importance of fall related solutions increases as the world population ages. However, the relative rarity and variability of real-world fall incidence has greatly impeded the progress of fall prevention/intervention/mitigation research. It is impracticable to request the elderly to wear motion capture sensors all year round only to capture one instance of fall. Hence, systems that induce falls in a safe controlled environment are essential to progress our understanding of the neuromuscular mechanisms underpinning falls events. Trips and slips are the focus of this work as they represents the majority of externally induced falls [2].

Several efforts have been made to create a system to induce an ecologically valid trip event. The most common types of fall induction systems generally rely

*Correspondence: jker@ntu.edu.sg
[1]Nanyang Technological University, Rehabilitation Research Institute of Singapore, 11 Mandalay Road, #14-03, 308232 Singapore
Full list of author information is available at the end of the article

on instrumented treadmill systems to perturb a participant during walking gait trials [3, 4, 5, 6]. These treadmill systems allow for precise and accurate velocity control that conventional overground walking systems are not able to replicate. Obstacles and perturbations can also be rendered easily as many mechanisms can be hidden around and under the instrumented treadmill systems. Though there are obvious benefits for the use of instrumented treadmill systems within the falls literature, it is widely known that an individual's gait pattern changes when walking on a treadmill versus over ground. Differences in an individual's kinematics [7, 8, 9], joint moments and muscular activation [10, 11, 9] have been well documented. Additionally, control of the treadmill after fall onset is critical to replicate true fall dynamics. The treadmill must travel exactly to the speed of the recovery limb to prevent artificially widening or narrowing their Base of Support (BoS).

Another type of trip induction system uses overground walking to generate more realistic real-world type falls. However, the engineering problem with these types of systems are that they need to account for the changes in the subject's linear position during walking gait. Multiple hidden obstacles have been built to induce trips along a fixed pathway [12, 13, 14, 15]. Since different gait phases induce different recovery strategies, these obstacles have to be densely packed to synchronise the simulated trip with the correct gait phase [12, 16]. Although the varying gait patterns can be accounted for with these obstacles, only one obstacle can be engaged at every instance - rendering this fall induction system to be inefficient cost expensive to implement, making them a non-practical research solution for laboratories globally, particularly those located in economically developing countries. A more cost effective method to this engineering problem is to develop a brake and motor system, in place of the multiple obstacles, to induce falls over a distance[17]. Nonetheless, regardless of the fall induction mechanisms used, the system must utilise an overhanging railing harness system for subject's safety, limiting its use to a designated location. Moreover, this overhanging railing harness system, which can have high inertia, alters the gait mechanics of the subject/patient under investigation.

Slip experiments commonly depended on using a split-belt treadmill [18] or a motorised floor plate [19] to provide the sudden gain in acceleration during a slip. However, the limited actuation distance of these devices mean that slipping is only allowed over a short distance. Once the motorised plate or treadmill stops, the subject can generally regain stability immediately, unlike a real-world slip scenario where velocity is slowly decreased. Even if the deceleration of the motorised plate or treadmill are controlled, it is difficult to match the intended joint kinematics. Furthermore, as previously mentioned, treadmill-walking changes the gait mechanics of the subject, arguably preventing the recording of a true transition from walking to slipping. A sliding plate [20] performs better in replicating a true slip scenario, but they are typically constraint by their sliding distance and the synchronisation of the leg touchdown position. Another method of inducing slips relies on sliding over a slippery surface [21, 22, 23]. This method replicates the true slipping scenario, but similar to a trip, they are constrained to a high inertia overhanging harness which can prevent the recording of a true transition from walking to slipping.

To the best of our knowledge, there exists one fall inducing robot for overground walking that allows changing heading angle and does not constraint the walking path [24]. This robot induced fall-like imbalance by providing perturbation at the pelvis. However, this method of fall induction bypasses the lower limbs reactive responses that are present in real-world fall scenarios. In addition, the changes in the dynamics of the lower limbs caused by obstacles and slippery surfaces are disregarded. Therein, they can affect an individual's falls recovery strategy. For example, a leg that encountered an obstacle during a trip will experience sudden deceleration and hence, the user would likely require more time to widen their BoS. Instead of arresting the leg movement during a trip, the forward pelvis perturbation from the robot may actually assist the subject to widen their BoS, resulting in improved stability.

The purpose of this research is to develop a Fall Inducing Movable Platform (FIMP). It is innovated for realistic fall induction in efforts to induce more realistic real-world falls scenario (Fig. 1). FIMP has the following characteristics:

- Allows change in heading angle, velocity and other gait patterns.
- Provides usage in a variety of relatively level ground without space constraints.
- Minimises mechanical inertia induced by the safety harness system applied to the subject.
- Induces more ecologically valid falls via ankle perturbations.
- Induces trip and slip with the same system.
- Creates a random, unexpected perturbation.

The design and methodology of FIMP is described in this paper, starting with the hardware, followed by the software. Additionally, experiments have been conducted to determine the transparency and kinematic effects of the trip and slip mechanisms of FIMP. Only trips and slips inducing capabilities were developed for

this generation of FIMP system as they are the most common types of real-world fall scenarios [25, 26, 2].

It can also be argued that an additional drawback of other publications in this field of research was the analysis method previously used to analyse time varying perturbations. Therein, they do not analyse time varying or continuum human movement data as a time series, but multiple discrete or zero dimensional (0D) time points (e.g., maximum, minima, mean etc.). Here, a novel analysis tool called 1-Dimensional Statistical Parametric Mapping (SPM1D) is introduced for fall recovery analysis [27]. It was originally developed within the neuroscience field for the analysis of changes in brain activation differences in functional and Magnetic Resonance Imaging (MRI) scan [28]. SPM1D was recently validated in the journal of statistical software for the analysis of time normalised signals of human movement (i.e., kinematics and kinetics) [29], which makes it well suited for fall-related research.

Methods

Several engineering components were necessary to realise the development of the FIMP system:

- Mobile Platform
- Trip and Slip mechanism
- Subject following and support algorithm
- Gait phase detection algorithm
- User Interface and System Control

Mobile Platform

The mobile platform of FIMP had a dimension of 175cm long by 115cm wide by 208cm tall (Fig. 1). This dimension was qualitatively tested to minimise the footprint necessary to prevent the lower limbs from hitting the platform while mitigating the sense of claustrophobia.

Two motorised wheels were mounted along the central axis of the FIMP such that the wheels can rotate the FIMP with a zero turning radius. The 2 DC motors obtained from *Motion Tech Motor* had a power rating of 250W each, and came equipped with electromagnetic brakes. They were controlled via a Sabertooth 2x32 motor driver. The motor driver was configured in mixed mode, which accepted 2 inputs; one input signal that controlled the forward speed, and another that controlled the turning speed and radius via the wheels differential speed. Five caster wheels were placed around the platform to ensure stability during movement. A 24V, 35AH Lipo battery powered the entire system.

Trip mechanism

The trip scenario was induced via wire ropes attached to the ankle of the subject (green dotted circle in Fig. 1). The continuous movement of the legs during gait requires the wire ropes to be freely moving. However, these freely moving ropes were often slack and caused a delay between perturbation activation time to force output through the wires. This delay in force transfer can contribute to variability in the fall recovery motion, and creates the risk of uncontrolled tripping over the slack ropes. The solution to this problem was to mount a small power spring within the reel of the wire rope. This power spring constantly reels back with a constant torque, and thereby keeping the wire taut to the ankle.

Trips were induced via an electromagnetic brake connected to the ankle using a similar power spring attached wire rope. The brake was supplied from *SINFONIA* (ERS-260L) with 8Nm static friction torque (Fig. 2). When a trip scenario was required, the brake activates and generates up to $347.8N$ of force (Table 2). Otherwise, the brake remains powered off and the power spring pulls with a passive force of $3.0N$ and a dynamic force of $5.9N$ (Table 1).

Slip mechanism

The slip scenario was induced via a DC motor. This approach was chosen as the sudden acceleration for a slipping stance leg could only be achieved with a pull. The DC motor was obtained from *XaJong Co. Ltd* (M35SWG-2436), with continuous torque of 1Nm and speed of 3600rpm (Fig. 3). A wrap spring clutch from *Tiny-Clutch — Helander Product, Inc* was attached to the output of the DC motor to disengage the inertia of the motor from the power spring. The DC motor reels in the wire rope wound around the exterior shell of the power spring after engaging the clutch with $0.12Nm$ of torque. The maximum pulling force exerted by the slip assembly was $110.3N$ (Table 2). When the motor was disengaged, the passive tension force caused by the power spring was $1.0N$ and $3.5N$ dynamically (Table 1).

When conducting slip trials, the subject's walking pathway was covered with 2 layers of sliding sheet. The coefficient of friction between the 2 layers of sliding sheet was approximately 0.15 for both static and kinetic scenarios. This inclusion of sliding sheets replicated the true slip conditions, whereby the slip foot continues to slide forward even after the initial pull by the slip motor.

When both trip and slip assemblies were utilised together, subjects within FIMP will only feel an overall static tension of $2.0N$ and dynamic tension of $2.4N$ around their ankle as the opposing forces cancel each other. Hence, during either trip or slip experiments, both assemblies were attached to the ankle.

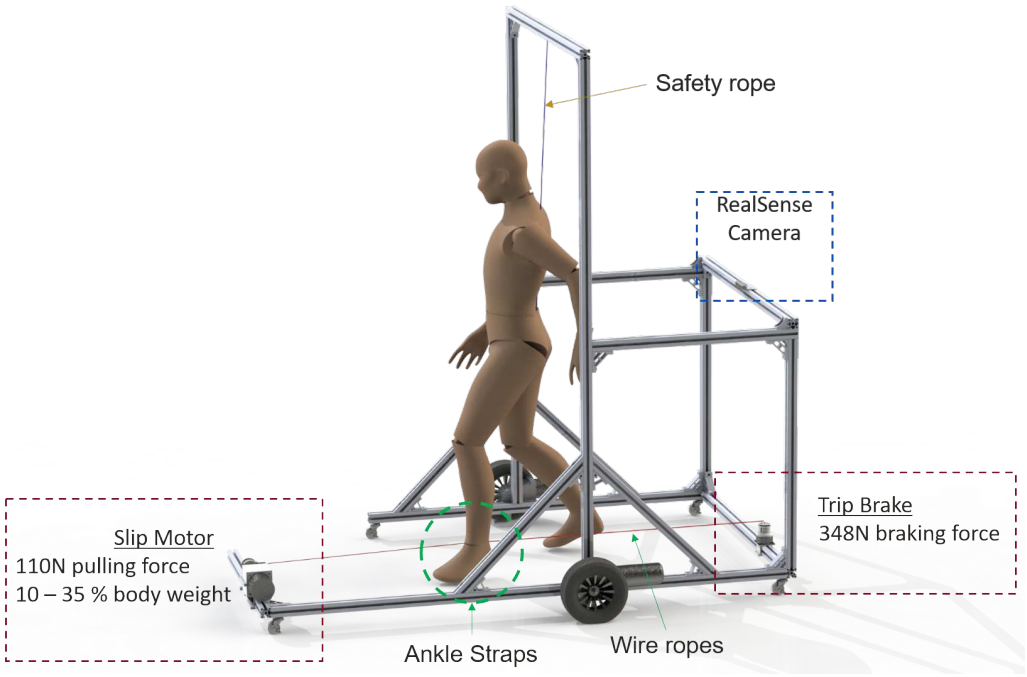

Figure 1 Fall inducing movable platform (FIMP). The structure was made from 40cm X 40cm aluminium profiles. A brake was used for trips induction and DC motor for slips. Slips and trips were induced on the left leg via wire rope (green dotted circle). A RealSense camera mounted at the back of the platform allowed for subject following technology. The safety rope mounted across the top of the platform prevented fall impact while having zero inertia on the subject during walking.

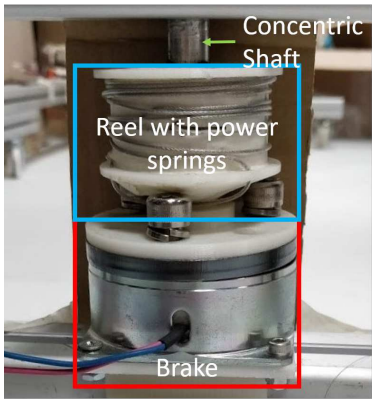

Figure 2 The trip brake mounted on FIMP with a concentric shaft keeping the reel with constant force spring centred.

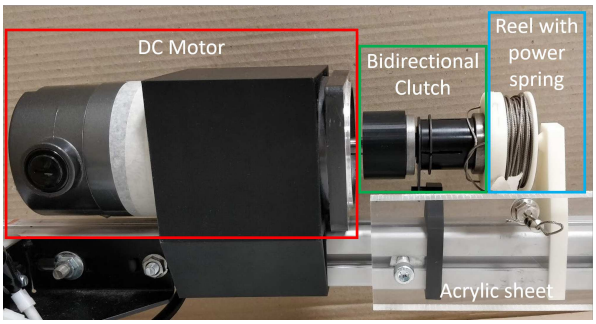

Figure 3 The slip motor was mounted horizontally with its output shaft connected to a bi-directional clutch and finally to a constant force spring. To prevent over-reeling of the motor, a thick acrylic sheet with a hole prevented the cable endings from being reeled in. The hole also guided the wire rope into the reel getting tangled. A fuse was added in series with the motor to prevent excessive torque.

Table 1 Cable tension force before fall mechanism activation

	Trip Spring	Slip Spring
Static Force (N)	3.0	1.0
Dynamic Force (N)	5.9	3.5

Table 2 Maximum cable tension force after fall mechanism activation

	Trip Brake	Slip Motor
Max Force(N)	347.8	110.3
ON Duration (ms)	250	750

Subject Follower Algorithm

The subject follower algorithm allowed the user to walk around a variety of level ground while changing heading angle, velocity and gait pattern. It also reduced the perceivable inertia of safety harness as it was attached to the top of the following platform.

Manually pushing the platform was acceptable, but it causes varying degrees of fall severity as the moving platform will alter the pulling and braking force of the fall mechanisms if they were not synchronised. Hence, the subject follower algorithm is important to obtain a constant fall severity. FIMP was motorised with 2 wheels along the central axis to allow for seamless synchronisation of the fall mechanism(s) and the movement of the platform.

An Intel RealSense Depth Camera D435 was used to estimate the position of the subject within FIMP. Usage of the depth camera allowed for subject tracking without any physical contact, eliminating any interference with normal walking gait. The camera was mounted at the back of FIMP, pointing directly forward at the centre of FIMP (Fig. 4). The estimated distance of the subject from the camera was obtained by averaging all the depth pixels of the camera. A Proportional Derivative (PD) controller controlled the speed of the motorised wheels to maintain a distance of 60 cm from the camera.

The angle of 2 vectors (subject's average pixel centre to camera, and FIMP's forward axis, Fig. 5) was used to re-centre the subject within FIMP when the subject turned. The angle was input into another PD controller to control the differential speed of two wheels via a motor driver.

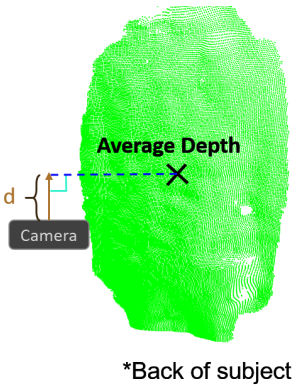

Figure 4 Calculation of forward distance for the subject follower algorithm.

Gait Phase detection Algorithm

Different types of falls call for different neuromuscular recovery strategies. For trips, an elevating strategy is used when an easy to overcome external perturbation occurs at the early to mid-swing gait phase [12, 30]. When the obstacle or perturbation becomes large enough, a skipping strategy is utilised [31]. This is due to the perturbed leg being arrested from moving forward by the perturbation. Hence, the contralateral leg must skip forward to reinstate a suitable base

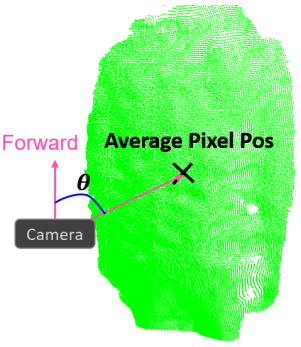

Figure 5 Calculation of orientation angle for the subject follower algorithm.

of support and regain stability. A lowering strategy is used during late-swing trips, where the perturbed leg lowers immediately after perturbation and an additional step is taken to clear the obstacle [12, 30].

Backwards falls are normally caused by slips that occur during the initial stance phase, as the contralateral stance leg is responsible for transferring the momentum of the body to the ground. When there is a lack of ground friction, the forward momentum pushes the stance leg forward, creating a slip. Slip's recovery strategy varies significantly with prior knowledge on the friction of the ground[16]. The initial slip recovery response will see the slipped foot immediately adopt a flat-footed configuration to the ground. Then, the contralateral leg is placed behind the Center of Mass (CoM) to provide a recovery moment. These responses require extending and flexing the perturbed and unperturbed leg respectively. Subsequent walking gait following the initial slip response will follow the *surfing* strategy which slides the swing foot forward rather than stepping off quickly during swing phase [16]. This is done to increase the contact area between the foot and the ground, thereby increasing frictional forces. Since the trip response differs based on tripped timing and slip must be triggered at initial stance phase, the correct identification of gait phase is important to induce the correct fall condition.

Two Inertial Measurement Unit (IMU)s were placed on the torso and left thigh of subjects to detect their body dynamics. Heading angle from the torso IMU's orientation vector were used to reorient the left thigh IMU's sagittal plane angular velocity and orientation output. Subsequently, these 2 axes (reoriented thigh IMU's angular velocity and orientation output) were dual-passed through a low-pass and high-pass Butterworth filter with cut-off frequency at 3Hz and

0.4Hz respectively. The Levenberg Marquardt Algorithm (LMA) was used to fit the filtered axes into a unit sine wave (sine wave with constant magnitude and offset). Finally, gait phase angle was calculated by doing an inverse tangent of the filtered and fitted sagittal plane's orientation over the angular velocity.

User Interface and System Control

Integration of the system is as shown in Fig. 6. The subject follower algorithm ensured that the platform follows the subject around. Upon a randomised triggering of a button from the investigator, the microcontroller (Raspberry Pi 3B+) automatically started the gait phase identification process. The gait phase angle was separated into 20 equal segments from $-\pi$ to π for easy segmentation of the gait phase. Once the gait phase has entered the pre-selected segment for the corresponding induced fall, the desired fall mechanism activates and FIMP stops. This induced a forward trip or a backwards slip depending on which fall inducing mechanism was used. Subjects were instructed to recover from the perturbation as fast as they could and stand straight after the fall. An emergency stop button was wired between the Lithium polymer battery power source and the wheels and fall inducing mechanism.

The automatic triggering of the fall mechanisms based on detected gait phase solved the problem of inducing different fall recovery strategies. Moreover, the stopping of FIMP and the fall mechanisms can now be synchronised.

The types of fall recovery strategies induced by FIMP are listed in Table 3. All the listed fall types were evaluated in this research except for the elevating strategy. This is due to the short time frame available to perturb and release the perturbed leg in order to reliably induce elevating strategy. More work will be conducted in the future to optimize the activation duration before the elevating strategy can be studied.

Table 3 Types of fall induced by FIMP

Fall types	Gait Phase	Fall mechanism	Activation Timing (ms)
Elevating Strategy	Early-Mid Swing	Brake	<250
Skipping Strategy	Early-Mid Swing	Brake	250
Lowering Strategy	Mid-Late Swing	Brake	400
Slip	Early Stance	Motor	250

Experimental Protocols

All trials were approved by the Institutional Review Board of Nanyang Technological Universtiy (IRB-2018-08-006). The gait phase detection system relied only on IMUs placed anteriorly on the subject's left thigh and torso, although other IMUs on the right thigh and shanks were also present. The IMUs were obtained from *Yost Labs*, and they were connected to a central micro-controller (Raspberry Pi 3b+) using a USB hub. A mean sampling rate of 333Hz was obtained after using Yost Labs proprietary Q-Comp filter. Each sample for gait analysis consisted of the body's local acceleration, local angular velocity and global quaternion orientation output. The entire gait phase detection system was attached to a big Velcro belt, which was worn around the subject's waist (Fig. 7). The waistband was tightened to the level where it did not slide down and yet remained sufficiently loose to allow for comfortable hip and lumbar flexion.

16 Qualysis Miqus M3 mocap cameras and 2 video cameras were used to track and capture subject's motion. The cameras were configured to sample at 200Hz. 53 Markers were placed on the L/R (Left and Right) Forehead, L/R Back head, clavicle, sternum, C7, right back, T10, L/R shoulder, L/R upper arm, L/R elbow, L/R forearm, L/R dorsal tubercle of radius, L/R styloid process of ulna, L/R middle finger's metacarpophalangeal joint, L/R anterior superior iliac spine, L/R posterior superior iliac spine, L/R thigh (4 markers), L/R lateral knee epicondyle, L/R tibia (4 markers), L/R ankle medial malleolus, L/R ankle lateral malleolus, L/R heel and finally L/R middle toe metacarpophalangeal joint (Fig. 7).

A total of 7 subjects (2 females and 5 males) were recruited for this experiment. They have an average age of 25 ± 0.94 years, average height of 168 ± 2.36 cm, average weight of 58 ± 6.24 kg, and an average Body Mass Index (BMI) of 20 ± 1.69. All subjects had no history of locomotor impairment, neurological impairment or cardiovascular diseases.

For each subject, they were asked to perform 3 types of walking trials at their preferred walking gait velocity along a straight path:

1) NormalWalking (NW) : 5 trials of walking without ankle cable and without harness.

2) StrapWalking (SW) : 5 trials of walking with attached ankle cable and with safety harness, but no fall.

3) Walking with attached ankle cable and harness with randomly induced falls:

- **3.1) MidSwing trip (MS)** : 3 trips initiated at mid-swing gait phase.
- **3.2) TerminalSwing trip (TS)** : 3 trips initiated at terminal-swing gait phase.
- **3.3) Slip (SL)** : 3 slips initiated at early-stance gait phase.

Ankle cable refers to the wire rope that was attached to the subject's ankle. This wire rope was kept taut by

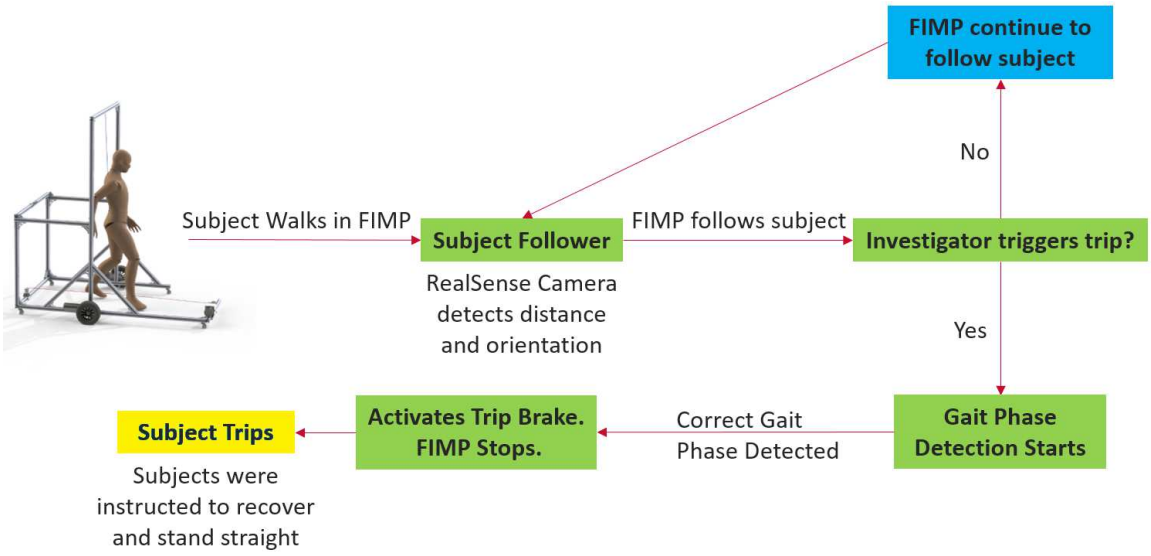

Figure 6 System control of FIMP. Subject starts walking in FIMP. RealSense camera detects the user's position and drives the wheels to follow the subject. As FIMP follows, it polls for investigator trigger via a button pressed for intention to trip the subject. When the button is pressed, the system automatically initiates the gait phase detection algorithm. Upon the correctly detected gait phase, the system immediately stops the wheels of FIMP and activates the trip brake. Subjects are instructed to recover and stand straight after the trip.

Figure 7 All subjects started by wearing a base Velcro suit, then a torso and seat safety harness and finally the Velcro belt with all the gait phase detection hardware. IMUs were placed on the torso, thighs and shanks of the subject, although only the left thigh and torso's IMU were used. Finally, reflective markers were secured onto the subject via the Velcro suit.

the power spring, and its force may influence the way the subject walks. Section studies the effect of FIMP during normal walking (i.e. system transparency).

Due to the space constraints of the laboratory and calibrated motion capture volume ($9m$ by $5m$ by $2m$), all the falls were induced 3 meters within the middle of the subject's walking pathway (6th to 9th step of a 15 steps pathway). Perturbations randomness were introduced by walking multiple trials and activating the falls only during some of the trials. An investigator constantly followed behind FIMP to activate the fall via the control switches and intervene if necessary by depressing the emergency stop button. When conducting slip trials, the low-friction sliding sheet mentioned above were placed along the walking pathway of the subject. Trips (MS and TS) and normal walking trials (NW and SW) were conducted on the normal laboratory floor surface.

All captured data were filtered with a 2^{nd} order Butterworth low pass filter at $6Hz$.

Results

FIMP Transparency

This section investigates the effect of FIMP (Transparency) during normal walking gait. An ideal fall inducing system should not affect the normal walking gait of the subject under any conditions. FIMP requires users to be attached to its fall inducing mechanisms via ankle straps which may affect the normal walking gait. Hence, the normal walking (NW, no ankle straps and no safety harness) trials were compared to the strap walking (SW, walking with straps and safety harness) trials to verify what influence, if any, the FIMP may have on the subject's walking gait. For this analysis, time varying sagittal plane hip, knee and ankle joint kinematics were compared using SPM1D.

Conventional methods of comparing different trials typically used 0D or discrete time points of a time varying signal like maximums, minimums, standard deviations, which we can argue are deemed unsuitable for falls type research and this experiment specifically. This is because the entire waveform is not being statistically analysed, predisposing research's from making both type 1 and type 2 errors with this analysis [32]. Therefore, a topological method for detecting field changes in smooth n-dimensional continua called SPM1D [27] was employed. Specifically, SPM1D analysis of t-test statistics (SPM1D{t}) allows for the time-normalised analysis of sagittal plane flexion joint angles at each point in the time series, which forms a statistical parametric map. The temporal smoothness based on the average temporal gradient can then be estimated using random field theory [27] to generate the test statistic threshold. Significance is achieved only when the value of the test statistic exceeds the test statistic threshold. Hence, two datasets with high time-varying variance require a breach at a high threshold to be classified as statistically different.

The stride of each gait cycle of every trial were segmented by heel strike. For every stride, it was normalized for fixed stance and swing phase duration. The stance phase was normalised to fit the first 60% of the gait cycle and the remaining 40% for the swing phase. The toe-off of each leg was used to demarcate the end of stance phase. The left and right legs were compared separately as the ankle strap was only attached to the left ankle during SW trials. A two sample t-test was conducted with SPM1D analysis, with an alpha threshold of 0.05. The relative effect NW versus SW SPM1D{t} was also presented in the format of a colour map for both combined and individual trials (Fig. 8 and Fig. 9). The colour map allows for readers to understand the relative effects of regions where statistical significance were observed. For t tests, the level of significance was separated into intervals of 1 standard deviation as t tests calculate the relative difference between 2 groups over their combined standard error of mean.

Left Leg

Results indicate that there was little to no differences between the hip and knee flexion kinematics of the left leg between NW and SW (Fig. 8). This implies that the ankle straps and safety harness did not affect the movement of the thigh and shank. On the contrary, there were significant differences in the ankle plantar/dorsi flexion kinematics for the left leg when the NW and SW conditions were compared. However, the magnitude of effect of the strap was not consistent among all the subjects, indicating that certain subjects were more influenced by the ankle straps heterogeneously. Even among those who were affected, this larger dorsiflexion is thought to have minimal effect on balance recovery during fall events. This is because the excess dorsiflexion happens during mid-swing, which does not generate any appreciable internal or external forces or torque experience on the subject. The only effect may be a slight increase in fatigue on the muscles responsible for dorsiflexion (e.g. tibialis anterior).

To ensure greater FIMP transparency and a greater resemblance to normal walking, it is still important to reduce the effect of the ankle straps. Several factors may contribute to the observed differences in ankle plantar/dorsiflexion. Firstly, the act of attaching the ankle straps requires interaction with the reflective markers on the ankle which may have affected their calibrated alignment. Secondly, the ankle strap can move during plantar/dorsiflexion of the swing phase, affecting the position of the shank malleolus markers, which were used to define the position of the ankle joint centre. Next, the tension force on the ankle strap may have require higher dorsiflexion to compensate for a lower toe clearance height. Lastly, the tightness of the ankle straps could have prevented the normal functioning of the ankle. Therefore, future research is recommended to determine the causal factors underpinning the observed differences. Guiding future research, it is speculated that the engineering solution to this problem is to improve the force characteristics of the power spring and improve methods to control the tightness of the ankle straps.

Right Leg

The right leg that did not have a strap attached to it shows no significant differences between NW and SW conditions for all lower limb joints (Fig. 9). This result also implies that the harness mounted on the movable FIMP did not affect the gait of the subject, and the method of using subject follower algorithm to reduce harness inertia is a success.

FIMP Terminal-Swing Tripping Effectiveness

Perturbations during the terminal-swing gait phase induced lowering recovery strategy [12], which corresponded to the lowering of the perturbed leg followed by the contralateral leg to overcome the obstacle (Fig. 10 and Additional file 1). This section examines the effect of the trip on the ipsilateral leg (perturbed left leg) and the contralateral leg (right leg). One-way repeated measure Analysis of Variance (ANOVA) with SPM1D were employed to identify the time instance when the perturbed gait cycle deviated from NW and SW. Again, the chosen alpha level was 0.05. Similar to the t tests conducted in the gait transparency section

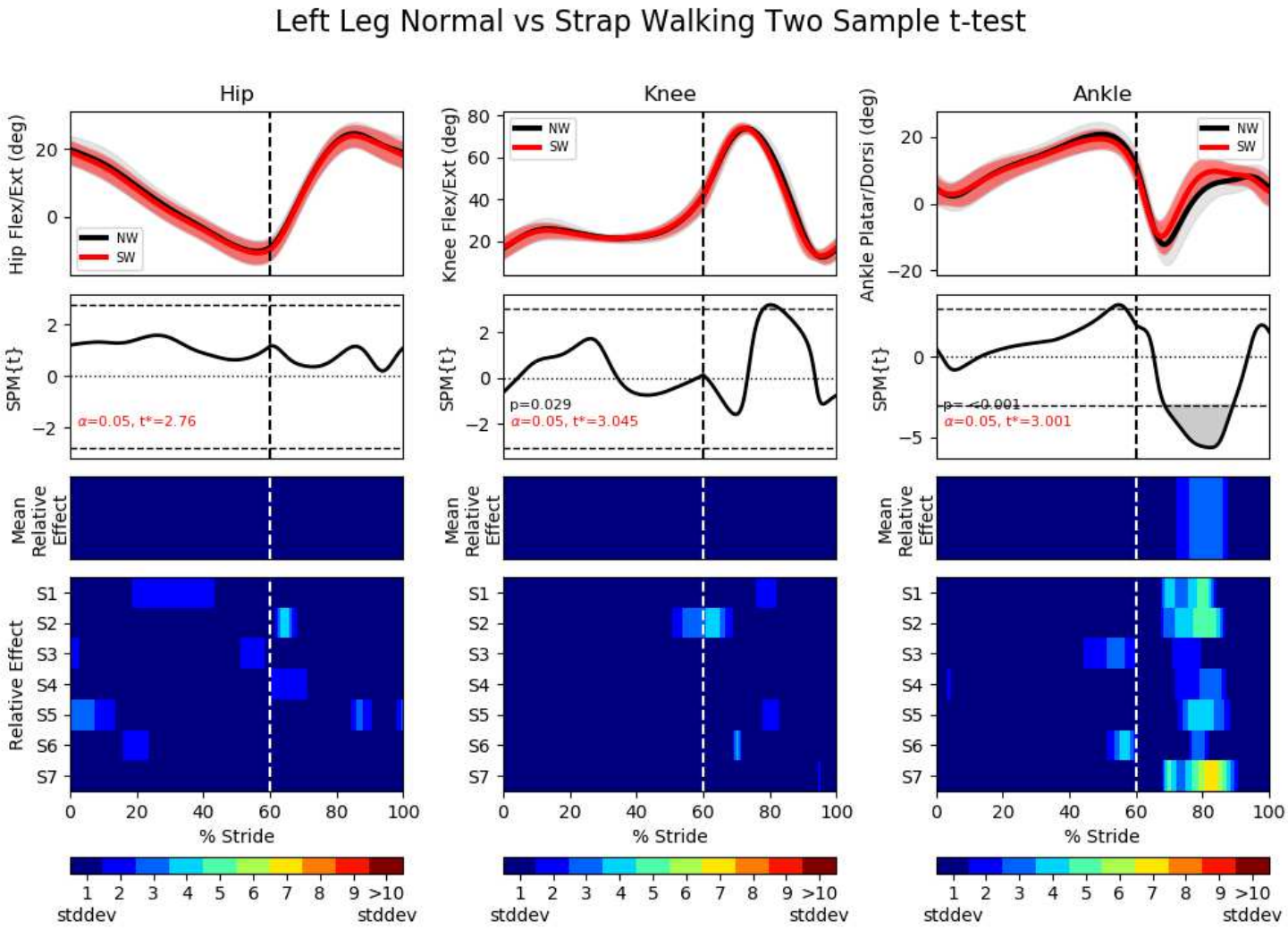

Figure 8 Comparison of NormalWalking (NW) vs StrapWalking (SW) trials for the left leg using SPM1D. The left leg is the leg with the ankle strap attached for fall induction. Top row indicates the mean hip, knee and ankle flexion angles for all subjects and standard deviation clouds; mean (± st.dev). Second row indicates the Two-sample t-test on the data in top row. The third and last rows show a colour map highlighting the t-test significant differences for the all subjects' combined and their individual NW vs SW trials. Significant differences are seen in the ankle joint during the mid-swing phase for the majority of the subjects. There are also differences found in the knee during the mid-swing phase, but it is less consistent among all the subjects.

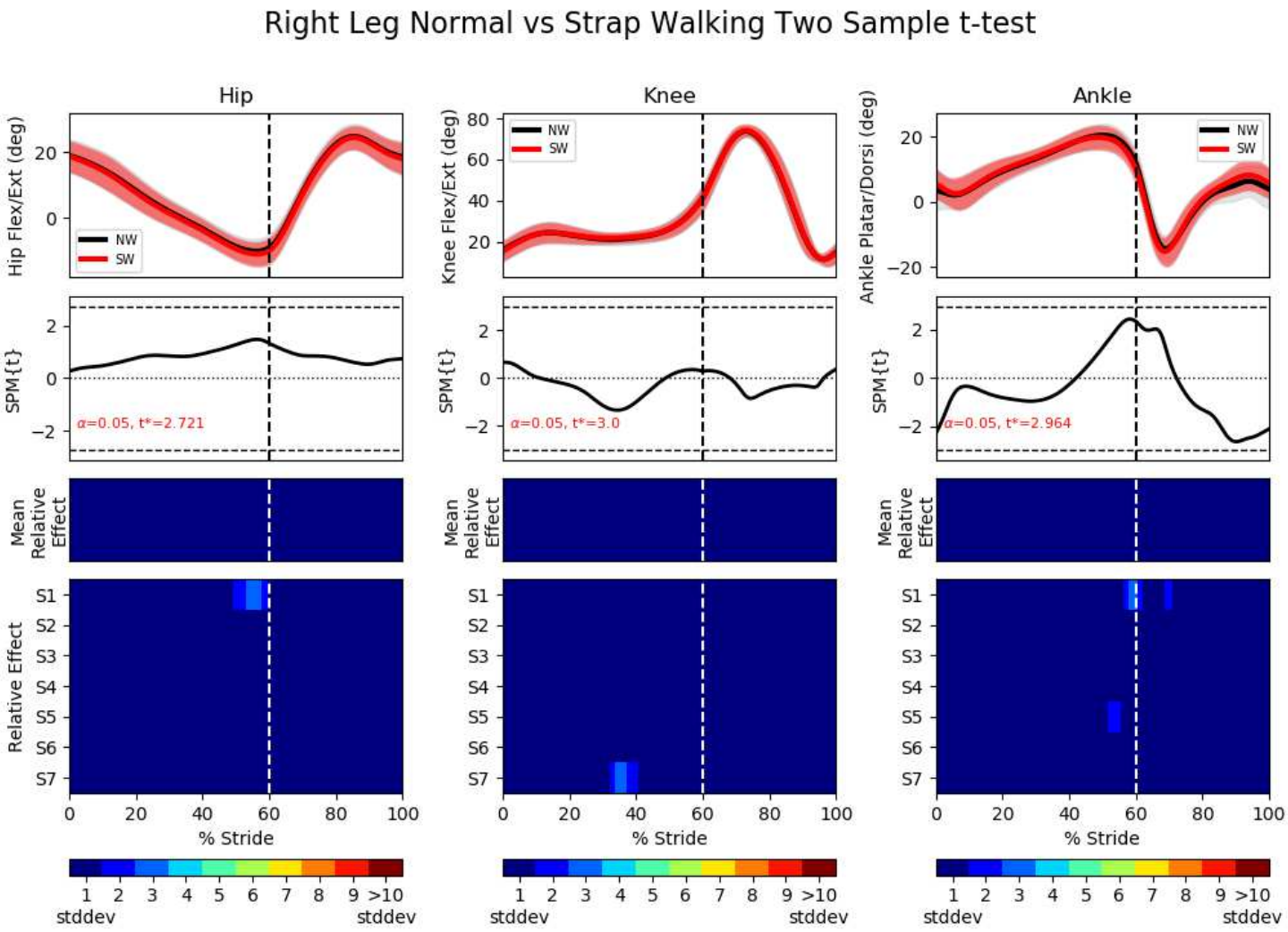

Figure 9 Comparison of NormalWalking (NW) vs StrapWalking (SW) trials for the right leg using SPM1D. The right leg is not attached to any ankle straps. Top row indicates the mean hip, knee and ankle flexion angles for all subjects and standard deviation clouds; mean ($\pm$ st.dev). The third and last rows show a colour map highlighting the t-test significant differences for the all subjects' combined and their individual NW vs SW trials. The last row shows the significant different effect size of individuals. No significant differences are found in any of the joints for the majority of the subjects

above, the ANOVA relative effect colour maps were also presented. However, the intervals used to visualise statistical significance were Mean Square of Error (MSE). This was used as the F value of ANOVA was calculated as the mean of group effects over MSE.

Left Leg

The gait cycles of the left leg containing the instances of perturbation were averaged for all subjects' TerminalSwing (TS) trip trials as shown in Fig. 11. Results show that the ipsilateral hip joint did not exhibit significant differences between NW and SW conditions. However, the knee joint experienced less extension, while the ankle joint underwent higher plantarflexion at the end of the swing phase.

The lack of difference at the hip joint is in-line with the perturbation occurring at the terminal-swing phase. During terminal-swing phase, the hip flexion muscles are contracted near the maximum flexed position to allow momentum to swing the passive knees forward. As perturbation is applied, the disturbance did not affect the hip joint as significantly as the knee and ankle joints because it is thought that the hip joint has higher stiffness created by its activated muscles.

The effect of the tripping mechanism was most evident in the knee joint during the terminal-swing phase. This is because, the perturbation force vector acts on the knee joint at a significantly larger moment arm than the ankle joint. The low stiffness knee joint caused by its passive muscles during swing phase also resulted in the large deviation from the normal trajectory during disturbance.

The ankle joint was less affected by the perturbation force due to the perturbation force proximity to the ankle rotation axis. However, the foot still had higher plantar-flexion angle than the normal trajectory at the end of the gait phase to increase the air-time of the body for widening of the contralateral limb. This higher plantarflexion has also been observed in other trip studies [33, 34].

Right Leg

The right leg gait cycles immediately after the left leg's perturbation were averaged for all subjects' TS trials (Fig. 12). The stance phase of the right leg happened concurrently with the swing phase of the left leg, which is where the perturbation was applied. Immediately after the perturbation, the contralateral right leg had to rapidly raise the thigh while the ipsilateral left leg extended the knee to cushion the trip impact, and plantarflexes the ankle to increase the time off the ground. This rise in hip flexion angle is observed in the second row of the SPM1D plot for the hip. Significant differences were found even before the swing phase has initiated (swing phase starts at 60% stride, demarcated by the vertical dotted line). Subsequently, the hip joint continued in its flexion trajectory to bring the thigh and shank forward, extending the body's BoS.

The right knee experiences higher than normal flexion as observed by the significant differences seen at the terminal-swing phase. This higher knee flexion was caused by shorter than normal swing phase, preventing normal knee extension. Consequently, the higher knee flexion angle allows more of the touchdown impact to be absorbed by the knee joint. The ankle had more pronounced plantarflexion at the initial swing phase in preparation for an earlier than usual heel strike, and also may be acting as a spring to absorb the higher touchdown impact.

Subject 7 walked with a pronounced upright fashion (similar to a ballroom dancer), leading to a walking posture with an elevated forward leaning angle as compared to other subjects. This caused the terminal-swing perturbation to severely affect this subject's knee kinematics as his thigh needed to be raised much faster to compensate for the faster falling momentum.

Discussion

The terminal-swing tripping system successfully induced the lower strategy as described in the literature [12, 30]. The induced trip kinematics and recovery strategies were replicated across subjects, suggesting that the FIMP system can induce ecologically valid terminal-swing trips. Future reliability based research is recommended

FIMP Mid-Swing Tripping Effectiveness

Perturbations during the mid-swing gait phase normally induced the elevating recovery strategy [12], corresponding to an immediate rise of the perturbed leg to overcome the obstacle (Fig. 13 and Additional file 1). However, in this experiment, the brake's activation timing was lengthened to arrest the leg's kinematics for the majority of the swing phase. This mimics situations where the swing leg gets tangled on some rope or is in contact with some tall obstacles that the elevated toe clearance alone cannot overcome. Therefore, the skipping strategy that generally accompanies harder to overcome obstacles was observed. Similarly, as per previous analyses, ANOVA with SPM1D analysis were used for statistical analysis. An alpha of 0.05 was implemented.

Left Leg

The gait cycles of the left leg with perturbations were averaged for all subjects' MidSwing (MS) trip trials and shown in Fig. 14. The results indicate that there were significant differences in all 3 joints during the swing phase. Due to the tripping mechanism activating at the early to mid-swing phase, the hip had lower

Figure 10 End-swing fall sequence (left to right) induced by the brake attached to the subject's ankle via a wire.

flexion throughout the majority of the swing phase. On the contrary, the knee joint experienced higher flexion angles during the mid to late swing phase. The ankle displayed significantly higher plantarflexion for the majority of the swing phase. The appearance of significant differences throughout the swing phase indicate that the tripping mechanism had successfully tripped the subject at the early to mid-swing phase.

The reduced hip flexion angle in the swing phase was caused by the tripping mechanism preventing the left leg from moving forward. This kinematic change was generally not observed in the terminal-swing trip because the hip joint has already reached the maximum flexion pose at the instance of trip. The hip flexion continues to increase slightly after the perturbation because of 1) the excessive forward momentum, 2) the forward leaning of the upper body and 3) the deactivation of the tripping brake only after 250 ms.

It was observed that the knee joint experienced a decrease in knee extension, similar to terminal-swing trip, but to a greater degree. This happened because the ankle was arrested much earlier than terminal-swing, preventing majority of the knee extension from occurring. Significant ankle plantarflexion occurred throughout the whole swing phase due to the need to reach for stable ground, even as the brake continued to hold onto the ankle.

It is hypothesised that the hip flexion angle will increase instead of decreasing (as compared to NW and SW) when the brake activation timing is shortened. It is believed the shortened brake activation will induce the elevating strategy where the perturbed leg rise above and over the obstacle. However, the knee will remain in the current elevated flexed position due to the forward leaning of the body, shortening the time to heel strike.

Right Leg

The gait cycles of the right leg immediately after the MS perturbation on the left leg were averaged across all subjects and shown in Fig. 15. Undeniably, there are significant differences in hip flexion angle, happening as early as the start of the swing phase. The knee joint experienced lower flexion during the swing phase and the ankle had a relatively constant joint angles throughout the entire gait cycle.

The hip joint showed a significant difference in the early stance phase because the early mid-swing perturbation on the left leg corresponded to the beginning of the stance phase on the right leg. As the perturbation occurred, the whole body leaned forward, exerting its entire body weight on the right leg alone. This caused excessive hip joint flexion during the stance phase. As the left leg remains immobilized by the brake, all subjects reduced their trip-induced, unwanted angular momentum by skipping the right leg forward. This skip was observed to widen the BoS and allowed stability to be regained.

There was no difference in the knee flexion angle during stance phase as the whole body pivoted on the ankle and skipped forward rather than bending the knees to absorb the unwanted momentum. During the swing phase (during the skip), reduced knee flexion was observed as the legs were pushing off at the beginning and were trying to touchdown as fast as possible at the end. It is believed this motor control strategy was adopted to achieve a wider BoS along with the increased hip flexion, making the dynamic system more stable

The ankle joint acted as the pivot for the whole body to lean forward during the stance phase. Additionally, the ankle joint is responsible for generating propulsion force during push off to allow for the skipping action to occur. This was observed by the elevated ankle plantarflexion during the end stance phase for push off. In the swing phase, all subjects over compensated for the larger plantarflexion during push off with a larger than normal dorsiflexion (seen by the valley during the ankle swing phase). However, most subjects quickly recover and revert back to normal swing kinematics.

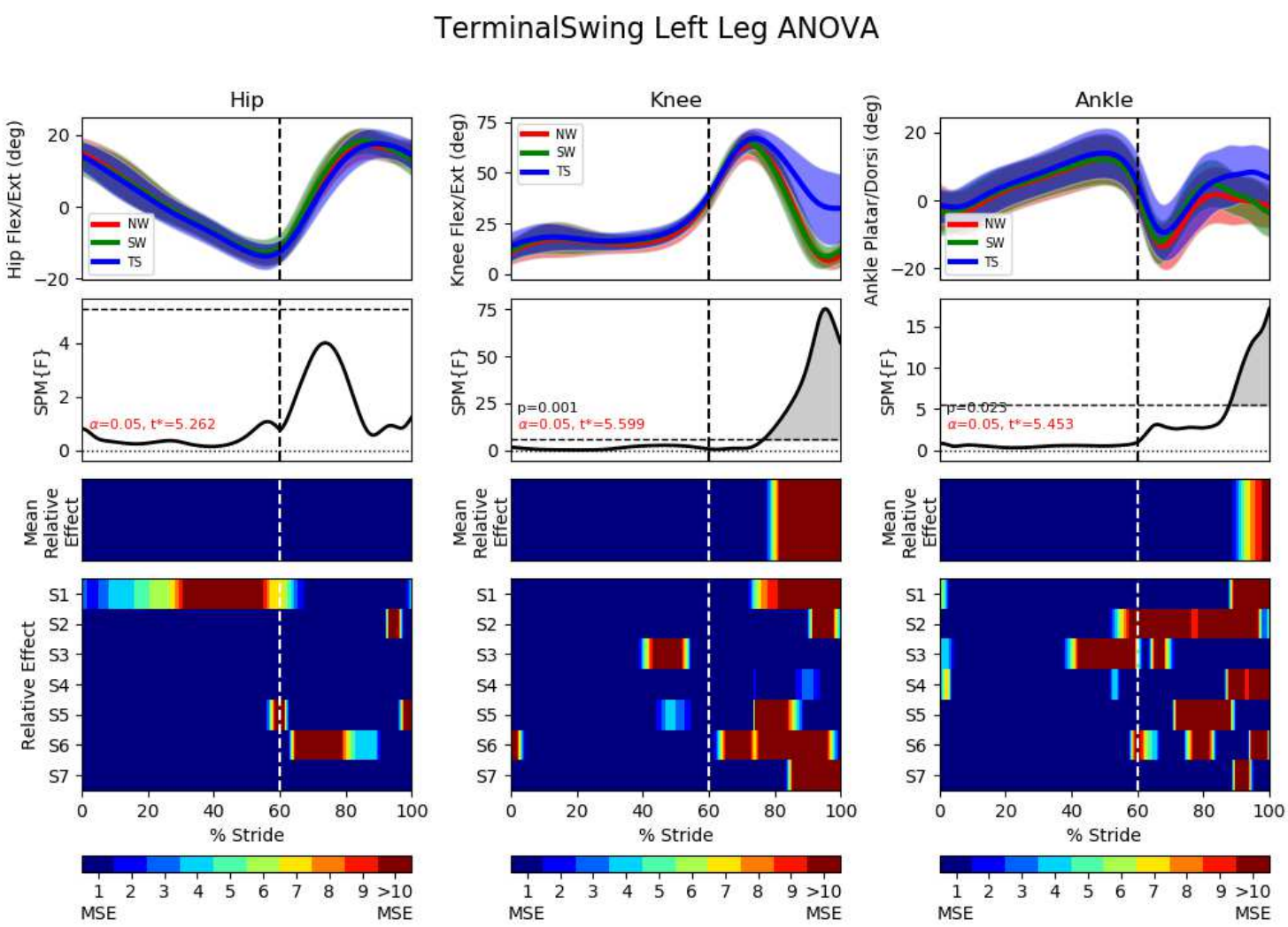

Figure 11 One-way repeated measure ANOVA comparison of NormalWalking (NW) vs StrapWalking (SW) vs TerminalSwing (TS) trials for the left leg with SPM1D. The left leg is attached to the ankle straps with a brake at the opposite end. Top row indicates the mean hip, knee and ankle flexion angles for all subjects and standard deviation clouds; mean ($\pm$ st.dev). Second row indicates the ANOVA test on the data shown in top row. Third row shows a colour map highlighting significant differences of the ANOVA result in second row. The last row shows the significant different effect size of individuals. Significant differences are observed in the knee and ankle joints near the terminal-swing phase.

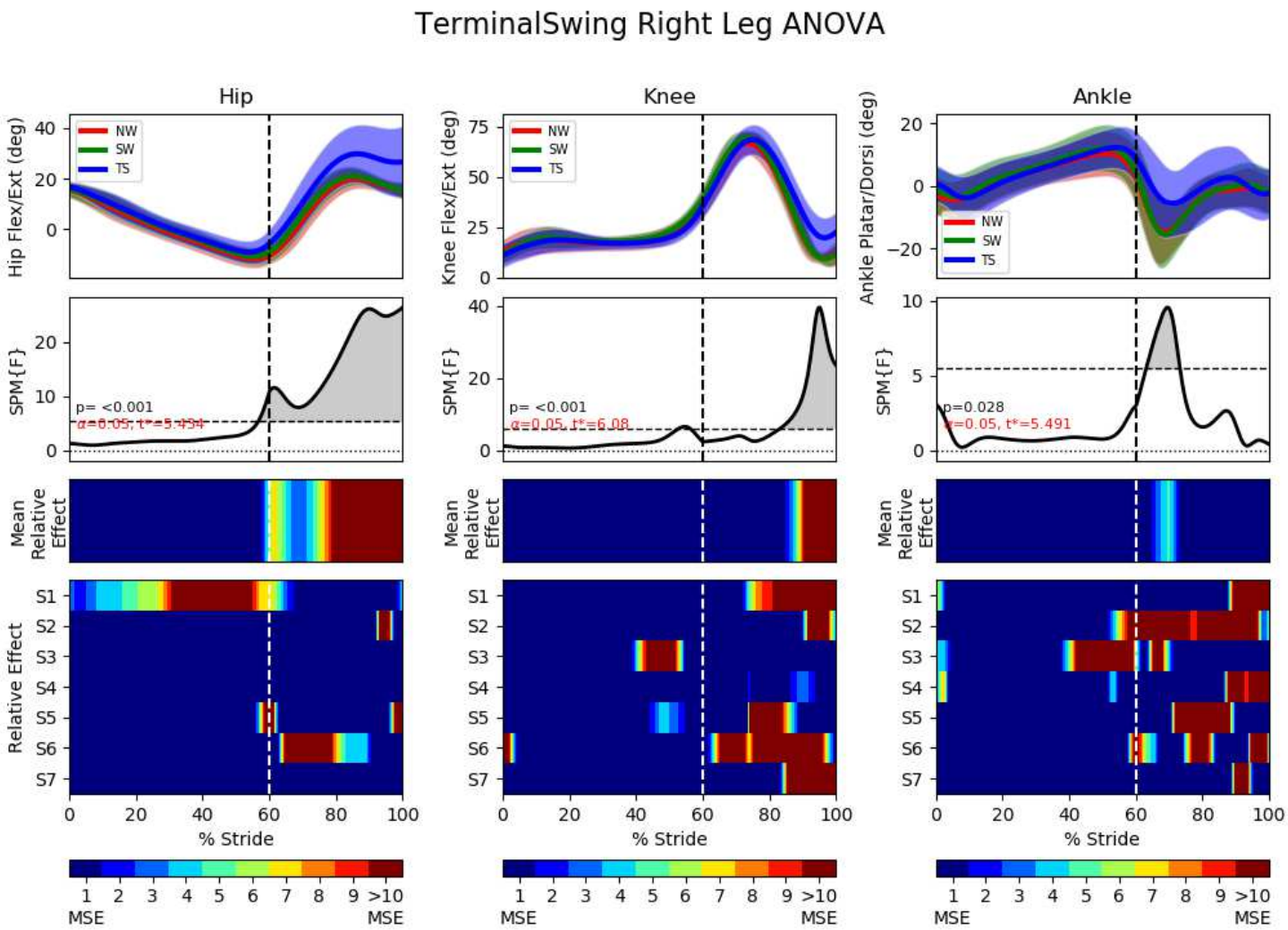

Figure 12 One-way repeated measure ANOVA comparison of NormalWalking (NW) vs StrapWalking (SW) vs TerminalSwing (TS) trials for the right leg with SPM1D. The right leg is attached not attached to any ankle straps. Top row indicates the mean hip, knee and ankle flexion angles for all subjects and standard deviation clouds; mean ($\pm$ st.dev). Second row indicates the ANOVA test on the data shown in top row. Third row shows a colour map highlighting significant differences of the ANOVA result in second row. The last row shows the significant different effect size of individuals. The hip joints have the most pronounced differences when comparing to NW and SW. The knee joint experiences lower extension angle at the terminal-swing phase, while the ankle joint has lower plantarflexion at the early swing phase.

Figure 13 Mid-swing fall sequence (left to right) induced by the brake attached to the subject's ankle via a wire.

Discussion

The induced mid-swing trip of the current experiment managed to immobilize the left ankle at the early to mid-swing phase. However, the recovery strategies employed did not follow the elevating strategy that is widely accepted as a mid-swing trip [35]. Instead, subjects skipped forward on their contralateral right leg to increase their BoS. This difference is likely attributed to the duration of the brake activation duration. This phenomenon has previously been reported but with the use of a different fall inducing method [31]. Since the current experiment arrested the ankle for 250 ms, the duration for fall recovery has already been expended by more than half. It is likely that certain proprioceptive reflex pathway senses the longer than normal perturbation and switch over to the skipping strategy. Nonetheless, these results showed that skipping strategy (a proven strategy of mid-swing trips) can be repeated, even among multiple subjects.

FIMP Slipping Effectiveness

Slip is induced at the beginning of early stance. Subjectively, subjects will only feel a loss of balance when sufficient body weight has been placed on the stance leg before pulling. Pulling at the late swing phase will induce a similar reaction to lowering strategy. Slip recovery likely requires subjects to stiffen their hip joint muscles [18], while adopting a flat-footed posture to reduce push-off's forward velocity [16] (Fig. 16 and Additional file 1).

Similarly, ANOVA with SPM1D analysis were used for statistical analysis.

Left Leg

The gait cycles of the left leg with perturbations were averaged for all subjects' slip trials (SL) and shown in Fig. 17. The results indicate that there were significant differences in all 3 joints during the swing phase. Since the slip motor mechanism pulled on the left leg at the beginning of the stance phase, significant differences were observed at the start of the gait cycle. The hip flexion angle remained relatively constant throughout the entire stance phase as hip muscles stiffened to prevent a backwards fall due to extension of the torso. Thereafter, during the swing phase, the left hip likely flexes to widen the BoS for stability while adopting a flat-footed surfing posture.

The knee joint began at a similar flexion angle as normal gait, but it flexes as slip was induced to lower the CoM for greater stability. The knee flexion was also caused by the upper body having a larger inertia than the lower limbs. As the upper body slid forward uncontrollably, the knees bent to absorb the unwanted forward velocity. The left knee maintained its flexion angle during the swing phase to adopt a surfing strategy which maximizes the ground to foot friction.

As the motor pulled on the ankle joint during the beginning of the stance phase, it increased the ankle plantarflexion. Thereafter, subjects immediately reacted to keep their foot flat on the ground to increase their friction with the ground, resulting in a similar trajectory as normal walking during the stance phase. However, significant differences were still observed in the swing phase because the subject has now adopted the surfing strategy, whereby the foot is continuously kept in constant contact with the ground. This caused the ankle to have a near zero flexion angle in the swing phase.

Right Leg

The gait cycles of the right leg that contained the instances of slip initiation on the left leg were averaged on all subjects and shown in Fig. 18. The most significant difference was observed near constant knee and ankle flexion angles during the swing phase. These changes were likely attributed to the adoption of the surfing strategy to decrease toe clearance and ankle push-off forward velocity. Reduced toe clearance allows subjects to touchdown sooner for stability and larger ground-foot frictional area. Minimizing the push-off forward velocity also reduces the chances of another slippage.

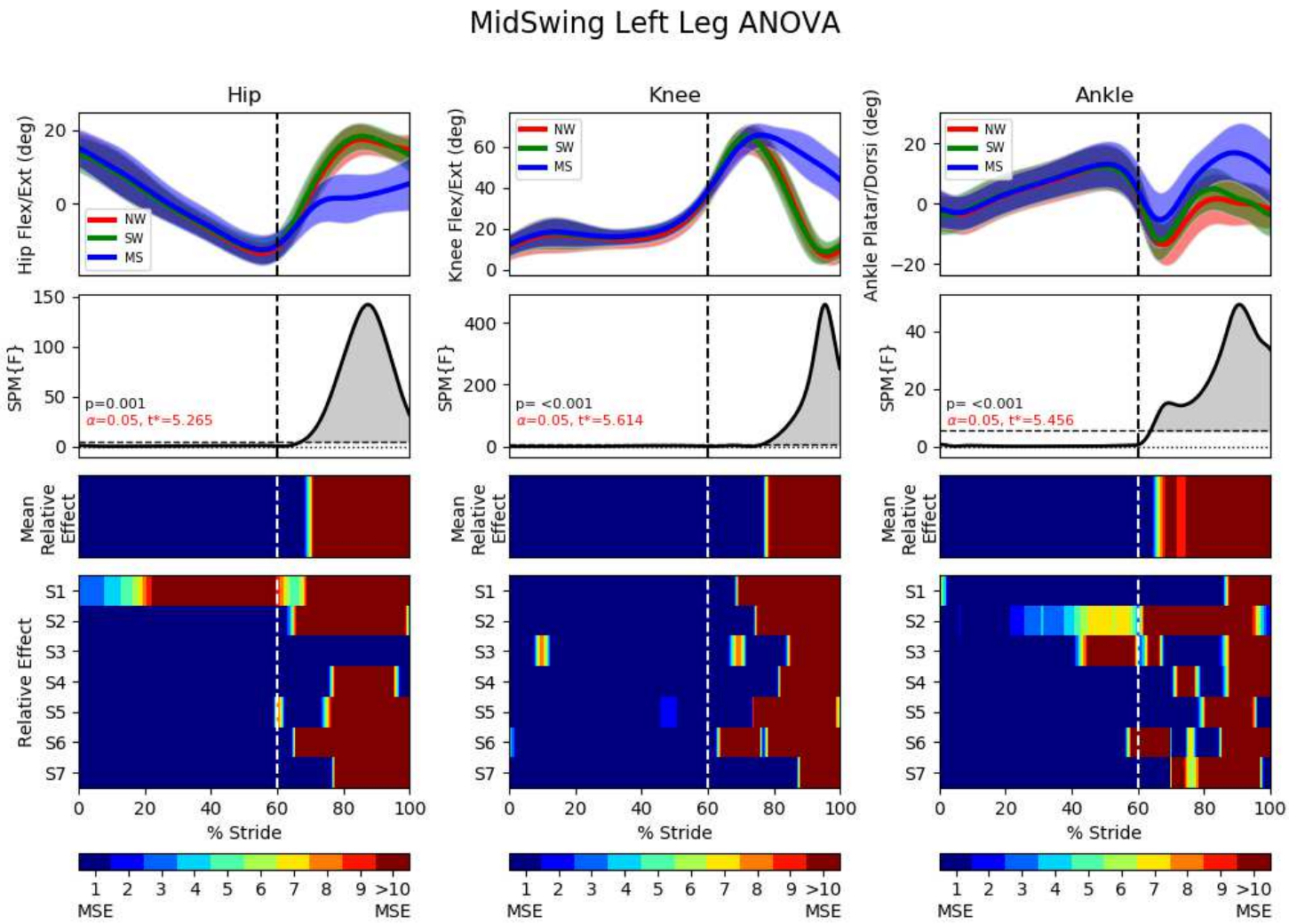

Figure 14 One-way repeated measure ANOVA comparison of NormalWalking (NW) vs StrapWalking (SW) vs MidSwing (MS) trials for the left leg with SPM1D. The left leg is attached to the ankle straps with a brake at the opposite end. Top row indicates the mean hip, knee and ankle flexion angles for all subjects and standard deviation clouds; mean (± st.dev). Second row indicates the ANOVA test on the data shown in top row. Third row shows a colour map highlighting significant differences of the ANOVA result in second row. The last row shows the significant different effect size of individuals. Significant differences are observed in the knee and ankle joints near the terminal-swing phase.

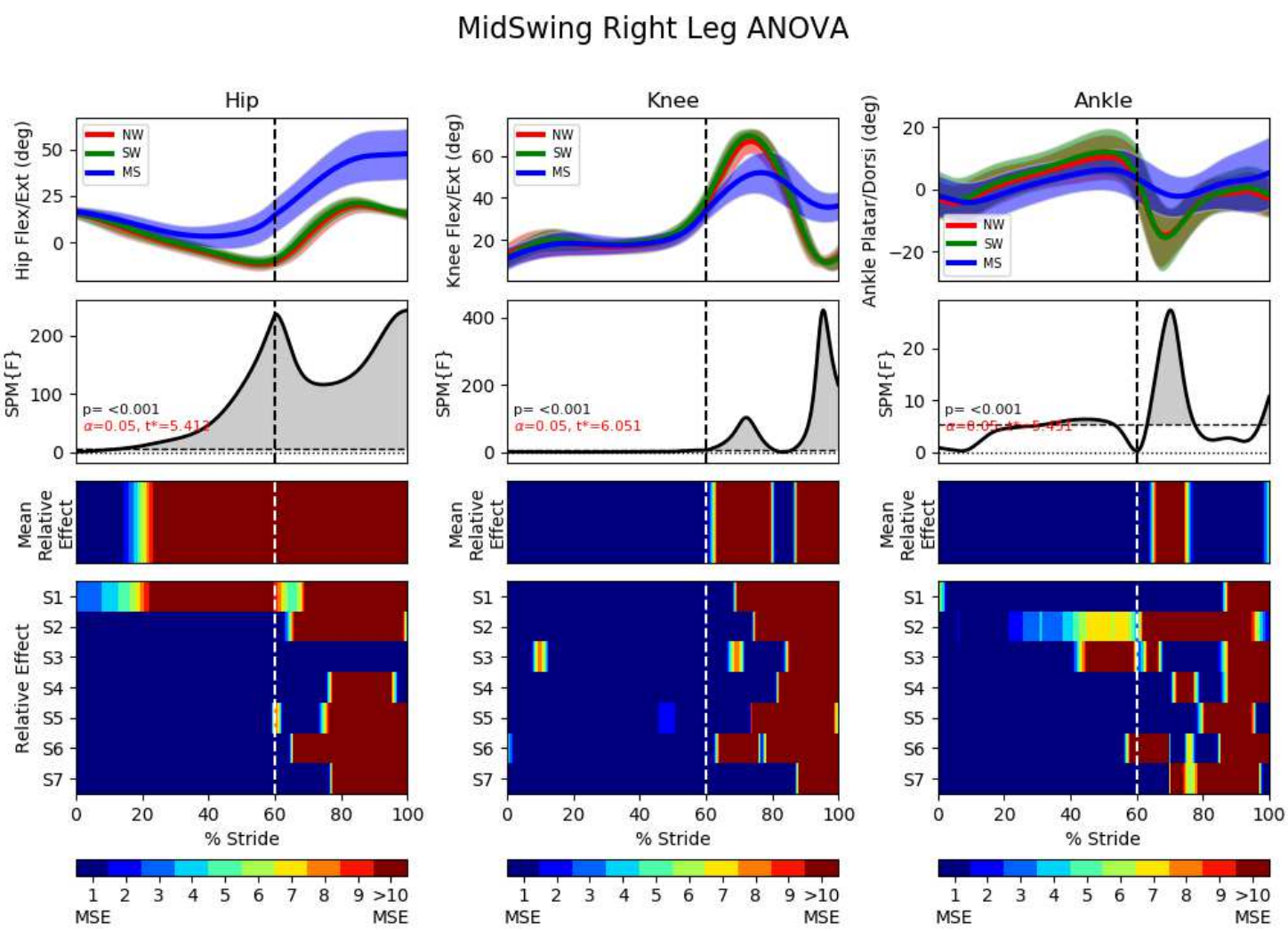

Figure 15 One-way repeated measure ANOVA comparison of NormalWalking (NW) vs StrapWalking (SW) vs MidSwing (MS) trials for the right leg with SPM1D. The right leg is not attached to any ankle straps. Top row indicates the mean hip, knee and ankle flexion angles for all subjects and standard deviation clouds; mean ($\pm$ st.dev). Second row indicates the ANOVA test on the data shown in top row. Third row shows a colour map highlighting significant differences of the ANOVA result in second row. The last row shows the significant different effect size of individuals. Significant differences are observed in the knee and ankle joints near the terminal-swing phase.

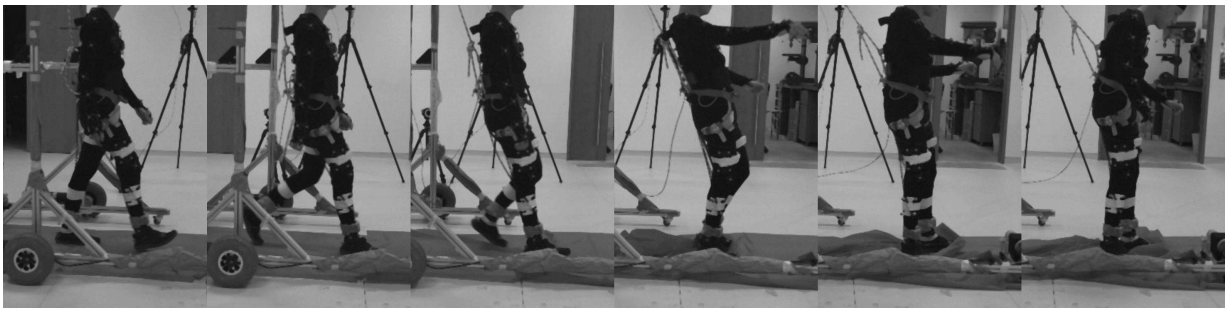

Figure 16 Slip fall sequence (left to right) induced by the motor attached to the subject's ankle via a wire. A low friction sliding sheet was placed on the ground to reduce foot to ground friction.

Anecdotally, subjects were observed to adopt a cautious walking gait, similar to the surfing strategy after the initial slip trial, as soon as they stepped onto the sliding sheet. This behaviour was also seen when individuals are walking on a slippery surface [16, 36], enforcing the ecological validity of this slip inducing mechanism. This change in gait pattern also created larger variability in all of the hip, knee and ankle joints, even during the stance phase, when slip has not occurred. This change in gait pattern was most significant in the ankle as the cautious walking gait requires a flat-foot sliding posture to increase ground-foot friction.

Discussion

The slip inducing mechanism of FIMP relies on both the motor for pulling force and the sliding sheet to reduce the friction of coefficient. The sliding sheet creates a near-slip sensation while the motor allows for accurate control of the slip timing. No slip has occurred on the sliding sheet without the activation of the slip motor.

After the initiation of the slip, subjects likely stiffened their joints to reduce the posterior movement of their CoM. Thereafter, the near constant hip, knee and ankle kinematics of the perturbed leg implies that subjects have adopted a flat footed surfing strategy to maintain high friction contact with the ground. Flat-footed strategy in stance allows for greater floor foot friction, while surfing strategy reduces the swing phase's toe clearance and push-off velocity to decrease chances of another slip.

Increased variability in recovery kinematics following the slip initiation was also observed when compared to other falls. This is likely due to the recovery actions being performed on the low-friction sliding sheet, causing multi-directional slippage which increases kinematics variability. Slipping during recovery is likely to happen during an ecologically valid slip as slippery surfaces are likely to extend over a wide area.

Conclusion

A novel fall inducing movable platform (FIMP) system was developed and showed to effectively induce both slips and trips during over ground walking gait conditions. Added benefit(s) to the system is that it does not limit its subjects to a constant heading angle, walking velocity or gait patterns, a notable limitation to treadmill-walking. Additionally, the light weight moving overhand safety harness system, enabled by the subject follower algorithm, did not inhibit the motion of the subjects with respect to their individualised movement pattern.

It is feasible to employ FIMP for fall studies. End-swing trips which induce lowering strategy can be reliably created, and the characteristic leg lowering and rapid rise of the contralateral leg to regain balance were easily observed. Skipping strategies were induced via mid-swing trips, although elevating strategy may be created with a shorter fall inducing time duration. During skipping strategy, the perturbed leg tried to straighten the knee while its hip was arrested. Since the perturbed leg cannot reach the ground with sufficient time, the contralateral leg needs to swing forward to widen the BoS. Slips were induced with FIMP, using the help of sliding sheets to reduce the ground-foot friction. During slips, both legs stiffened, and quickly transit to knees straightening to force a flat-foot configuration. Slip trials have much higher kinematics variability as the low-friction ground surface causes multi-directional slip of the lower limbs. Therefore, FIMP has proven to induce ecologically valid overground walking gait and falls, similar to those reported previously in the literature [12, 30, 16, 36, 35, 31].

The usage of SPM1D as an analysis tool provided researchers with the first ever quantifiable trip and slip reactive kinematics. SPM1D has also proven to be an invaluable statistical platform for visualising the changes in time-varying joint kinematics during various fall scenarios. Abnormalities with balance impaired subjects can now be targeted to the manage

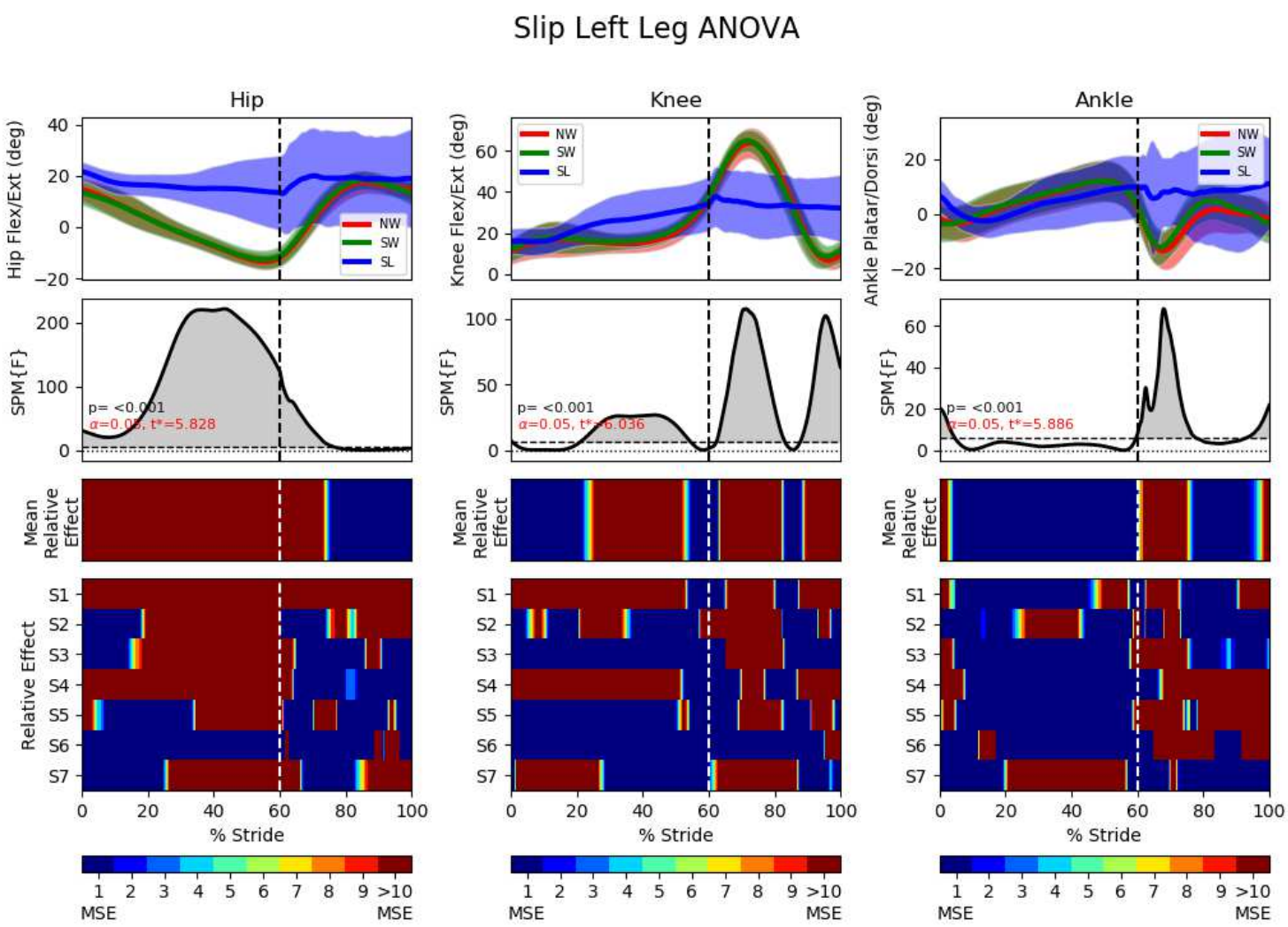

Figure 17 One-way repeated measure ANOVA comparison of NormalWalking (NW) vs StrapWalking (SW) vs Slip (SL) trials for the left leg with SPM1D. The left leg is attached to the ankle straps with a brake at the opposite end. Top row indicates the mean hip, knee and ankle flexion angles for all subjects and standard deviation clouds; mean ($\pm$ st.dev). Second row indicates the ANOVA test on the data shown in top row. Third row shows a colour map highlighting significant differences of the ANOVA result in second row. The last row shows the significant different effect size of individuals. All the joint angles are relatively constant as compared to NormalWalking. This indicates that stiffening of joints occur during slips.

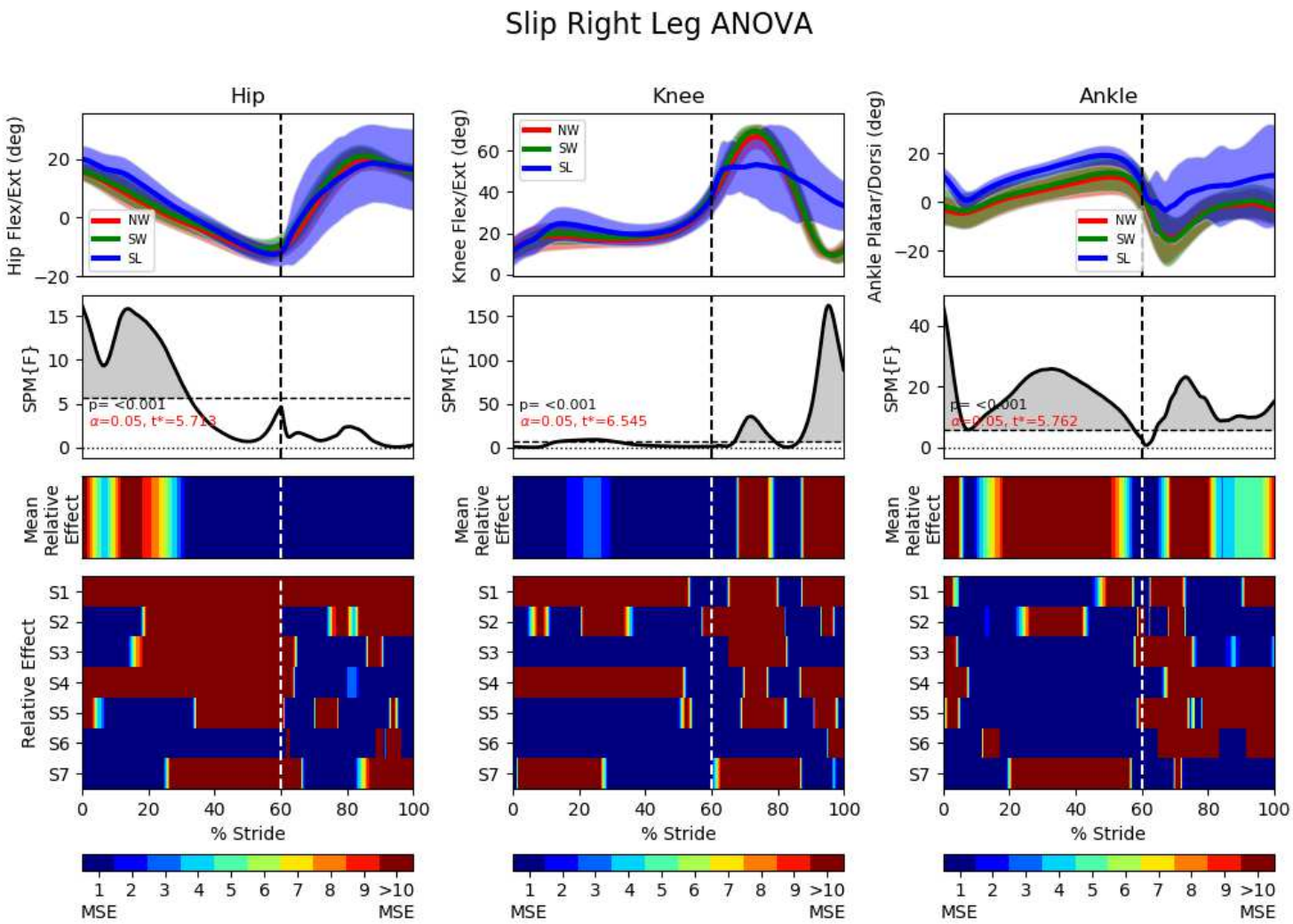

Figure 18 One-way repeated measure ANOVA comparison of NormalWalking (NW) vs StrapWalking (SW) vs Slip (SL) trials for the right leg with SPM1D. The right leg is not attached to any ankle straps. Top row indicates the mean hip, knee and ankle flexion angles for all subjects and standard deviation clouds; mean ($\pm$ st.dev). Second row indicates the ANOVA test on the data shown in top row. Third row shows a colour map highlighting significant differences of the ANOVA result in second row. The last row shows the significant different effect size of individuals. The right knee and ankle has a more constant joint angle throughout the swing phase, indicating the adoption of the surfing strategy (keeping foot flat and close to ground).

the true cause of their balance deficiency, such as weak muscles or slow reaction time.

Abbreviations
ANOVA: Analysis of variance; BoS: Base of Support; CoM: Center of mass; FIMP: Fall inducing movable platform; IMU: Inertial measurement unit; MSE: Mean square of error; PD: Proportional derivative; SPM: 1-dimensional statistical parametric mapping

Acknowledgements
The authors would like to thank the study participants for their participation and feedback; Chin Jiah Shin and Lim Zhen Yi for assisting in the proofreading and editing of the manuscript; and Tan Ri Liang for the assistance in tuning the fall mechanisms.

Funding
Funding for this work was provided by the Singapore Ministry of Health (Grant No: MOH/NIC/EIG01/2017).

Availability of data and materials
The dataset used and/or analysed during the current study are available from the corresponding author upon reasonable request.

Author's contributions
EJK was the main contributor to the conceptualisation, algorithm and hardware design, implementation, data acquisition, data processing, data interpretation and drafting of this manuscript. CJD assisted in data processing and interpretation of the graphs. WSK provided advice on the trip and slip mechanisms and implementation. AWT provided the initial project direction and resources, reviewed the algorithms and hardware. All authors read and approved the final manuscript.

Ethics approval and consent to participate
This study was approved by the Institutional Review Board of Nanyang Technological University (IRB-2018-08-006), and all methods were carried out in accordance with the approved study protocol. They subjects provided written informed consent before participation and consented to the publishing of their collected data.

Consent for publication
Written informed consent for publication was obtained from the participants involved in the study.

Competing interests
The authors declare that they have no competing interests.

Author details
[1]Nanyang Technological University, Rehabilitation Research Institute of Singapore, 11 Mandalay Road, #14-03, 308232 Singapore. [2]Tan Tock Seng Hospital, Centre for Advanced Rehabilitation Therapeutics, 11 Jalan Tan Tock Seng, 308433 Singapore.

References

1. Rubenstein, L.Z.: Falls in older people: epidemiology, risk factors and strategies for prevention. Age Ageing **35 Suppl 2**, 37–41 (2006). doi:10.1093/ageing/afl084. Rubenstein, Laurence Z Review England Age Ageing. 2006 Sep;35 Suppl 2:ii37-ii41.
2. Robinovitch, S.N., Feldman, F., Yang, Y., Schonnop, R., Lueng, P.M., Sarraf, T., Sims-Gould, J., Loughin, M.: Video capture of the circumstances of falls in elderly people residing in long-term care: an observational study. Lancet **381**(9860), 47–54 (2013). doi:10.1016/S0140-6736(12)61263-X. 23083889[pmid] Lancet
3. Schillings, A.M., Van Wezel, B.M.H., Mulder, T.H., Duysens, J.: Widespread short-latency stretch reflexes and their modulation during stumbling over obstacles. Brain Research **816**(2), 480–486 (1999). doi:10.1016/S0006-8993(98)01198-6
4. Owings, T.M., Pavol, M.J., Grabiner, M.D.: Mechanisms of failed recovery following postural perturbations on a motorized treadmill mimic those associated with an actual forward trip. Clinical Biomechanics **16**(9), 813–819 (2001)
5. Luciani, L.B., Genovese, V., Monaco, V., Odetti, L., Cattin, E., Micera, S.: Design and evaluation of a new mechatronic platform for assessment and prevention of fall risks. Journal of neuroengineering and rehabilitation **9**(1), 51 (2012)
6. King, S.T., Eveld, M.E., Martínez, A., Zelik, K.E., Goldfarb, M.: A novel system for introducing precisely-controlled, unanticipated gait perturbations for the study of stumble recovery. Journal of neuroengineering and rehabilitation **16**(1), 69 (2019)
7. Alton, F., Baldey, L., Caplan, S., Morrissey, M.: A kinematic comparison of overground and treadmill walking. Clinical biomechanics **13**(6), 434–440 (1998)
8. Riley, P.O., Paolini, G., Della Croce, U., Paylo, K.W., Kerrigan, D.C.: A kinematic and kinetic comparison of overground and treadmill walking in healthy subjects. Gait & posture **26**(1), 17–24 (2007)
9. Parvataneni, K., Ploeg, L., Olney, S.J., Brouwer, B.: Kinematic, kinetic and metabolic parameters of treadmill versus overground walking in healthy older adults. Clinical biomechanics **24**(1), 95–100 (2009)
10. Wank, V., Frick, U., Schmidtbleicher, D.: Kinematics and electromyography of lower limb muscles in overground and treadmill running. International journal of sports medicine **19**(07), 455–461 (1998)
11. Lee, S.J., Hidler, J.: Biomechanics of overground vs. treadmill walking in healthy individuals. Journal of applied physiology **104**(3), 747–755 (2008)
12. Eng, J., Winter, D., Patla, A.: Strategies for recovery from a trip in early and late swing during human walking. Experimental Brain Research **102**(2), 339–349 (1994). doi:10.1007/BF00227520
13. Pavol, M.J., Owings, T.M., Foley, K.T., Grabiner, M.D.: Gait characteristics as risk factors for falling from trips induced in older adults. Journals of Gerontology Series A: Biomedical Sciences and Medical Sciences **54**(11), 583–590 (1999)
14. Pijnappels, M., Bobbert, M.F., van Dieën, J.H.: Changes in walking pattern caused by the possibility of a tripping reaction. Gait & posture **14**, 11–18 (2001)
15. Wang, T.-Y., Bhatt, T., Yang, F., Pai, Y.-C.: Adaptive control reduces trip-induced forward gait instability among young adults. Journal of biomechanics **45**(7), 1169–1175 (2012)
16. Marigold, D.S., Patla, A.E.: Strategies for dynamic stability during locomotion on a slippery surface: effects of prior experience and knowledge. Journal of Neurophysiology **88**(1), 339–353 (2002)
17. Smeesters, C., Hayes, W.C., McMahon, T.A.: Disturbance type and gait speed affect fall direction and impact location. Journal of biomechanics **34**(3), 309–317 (2001)
18. Monaco, V., Tropea, P., Aprigliano, F., Martelli, D., Parri, A., Cortese, M., Molino-Lova, R., Vitiello, N., Micera, S.: An ecologically-controlled exoskeleton can improve balance recovery after slippage. Scientific Reports **7** (2017)
19. Tang, P.-F., Woollacott, M.H.: Inefficient postural responses to unexpected slips during walking in older adults. The Journals of Gerontology Series A: Biological Sciences and Medical Sciences **53A**(6), 471–480 (1998)
20. Yang, F., Pai, Y.-C.: Correction of the inertial effect resulting from a plate moving under low-friction conditions. Journal of biomechanics **40**, 2723–2730 (2007). doi:10.1016/j.jbiomech.2006.12.008
21. Chambers, A.J., Cham, R.: Slip-related muscle activation patterns in the stance leg during walking. Gait & posture **25**(4), 565–572 (2007)
22. Liu, J., Lockhart, T.E.: Age-related joint moment characteristics during normal gait and successful reactive-recovery from unexpected slip perturbations. Gait & posture **30**(3), 276–281 (2009)
23. Parijat, P., Lockhart, T.E.: Effects of moveable platform training in preventing slip-induced falls in older adults. Annals of biomedical engineering **40**(5), 1111–1121 (2012)
24. Olenšek, A., Zadravec, M., Matjačić, Z.: A novel robot for imposing perturbations during overground walking: mechanism, control and normative stepping responses. Journal of neuroengineering and rehabilitation **13**(1), 55 (2016)
25. O'neill, T., Varlow, J., Silman, A., Reeve, J., Reid, D., Todd, C., Woolf, A.: Age and sex influences on fall characteristics. Annals of the rheumatic diseases **53**(11), 773–775 (1994)
26. Berg, W.P., Alessio, H.M., Mills, E.M., Tong, C.: Circumstances and consequences of falls in independent community-dwelling older adults. Age and ageing **26**(4), 261–268 (1997)
27. Pataky, T.C.: One-dimensional statistical parametric mapping in python. Computer methods in biomechanics and biomedical engineering **15**, 295–301 (2012). doi:10.1080/10255842.2010.527837

28. Penny, W.D., Friston, K.J., Ashburner, J.T., Kiebel, S.J., Nichols, T.E.: Statistical Parametric Mapping: the Analysis of Functional Brain Images, 1st edn. Academic Press, Cambridge, Massachusetts (2007)
29. Pataky, T.C.: Rft1d: Smooth one-dimensional random field upcrossing probabilities in python. Journal of Statistical Software **71**(7), 07 (2016)
30. Eng, J.J., Winter, D.A., Patla, A.E.: Intralimb dynamics simplify reactive control strategies during locomotion. J Biomech **30**(6), 581–8 (1997). Eng, J J Winter, D A Patla, A E Journal Article Research Support, Non-U.S. Gov't United states J Biomech. 1997 Jun;30(6):581-8.
31. Mitsuoka, K., Akiyama, Y., Yamada, Y., Okamoto, S.: Analysis of skip motion as a recovery strategy after an induced trip. In: Proc. and Cybernetics 2015 IEEE Int. Conf. Systems, Man, pp. 911–916 (2015). doi:10.1109/SMC.2015.167
32. Donnelly, C., Alexander, C., Pataky, T., Stannage, K., Reid, S., Robinson, M.: Vector-field statistics for the analysis of time varying clinical gait data. Clinical Biomechanics **41**, 87–91 (2017)
33. Marigold, D.S., Bethune, A.J., Patla, A.E.: Role of the unperturbed limb and arms in the reactive recovery response to an unexpected slip during locomotion. Journal of Neurophysiology **89**(4), 1727–1737 (2003)
34. Pijnappels, M., Bobbert, M.F., van Dieën, J.H.: Control of support limb muscles in recovery after tripping in young and older subjects. Experimental brain research **160**(3), 326–333 (2005)
35. Pijnappels, M., Bobbert, M.F., van Dieën, J.H.: Contribution of the support limb in control of angular momentum after tripping. Journal of Biomechanics **37**(12), 1811–1818 (2004). doi:10.1016/j.jbiomech.2004.02.038
36. Cham, R., Redfern, M.S.: Changes in gait when anticipating slippery floors. Gait & posture **15**(2), 159–171 (2002)

Additional Files

Additional file 1 — Fall Compilation video
A compilation video of different subjects being induced with terminal-swing trip, mid-swing trip and slip. All subjects were walking at their preferred speed and were instructed to stand straight immediately after their recovery. (MP4 5,191KB)

Additional file 2 — Post Hoc analysis
Post hoc analysis of terminal swing (TS), mid swing (MS) and slip (SL) versus normal walking (NW) and strap walking (SW). These post hoc analyses were conducted after performing the ANOVA as shown in Fig. 11, 12, 14, 15, 17, 18. Bonferroni correction was used to adjust the alpha value for the multiple comparisons. (PDF 1,439KB)

Figures

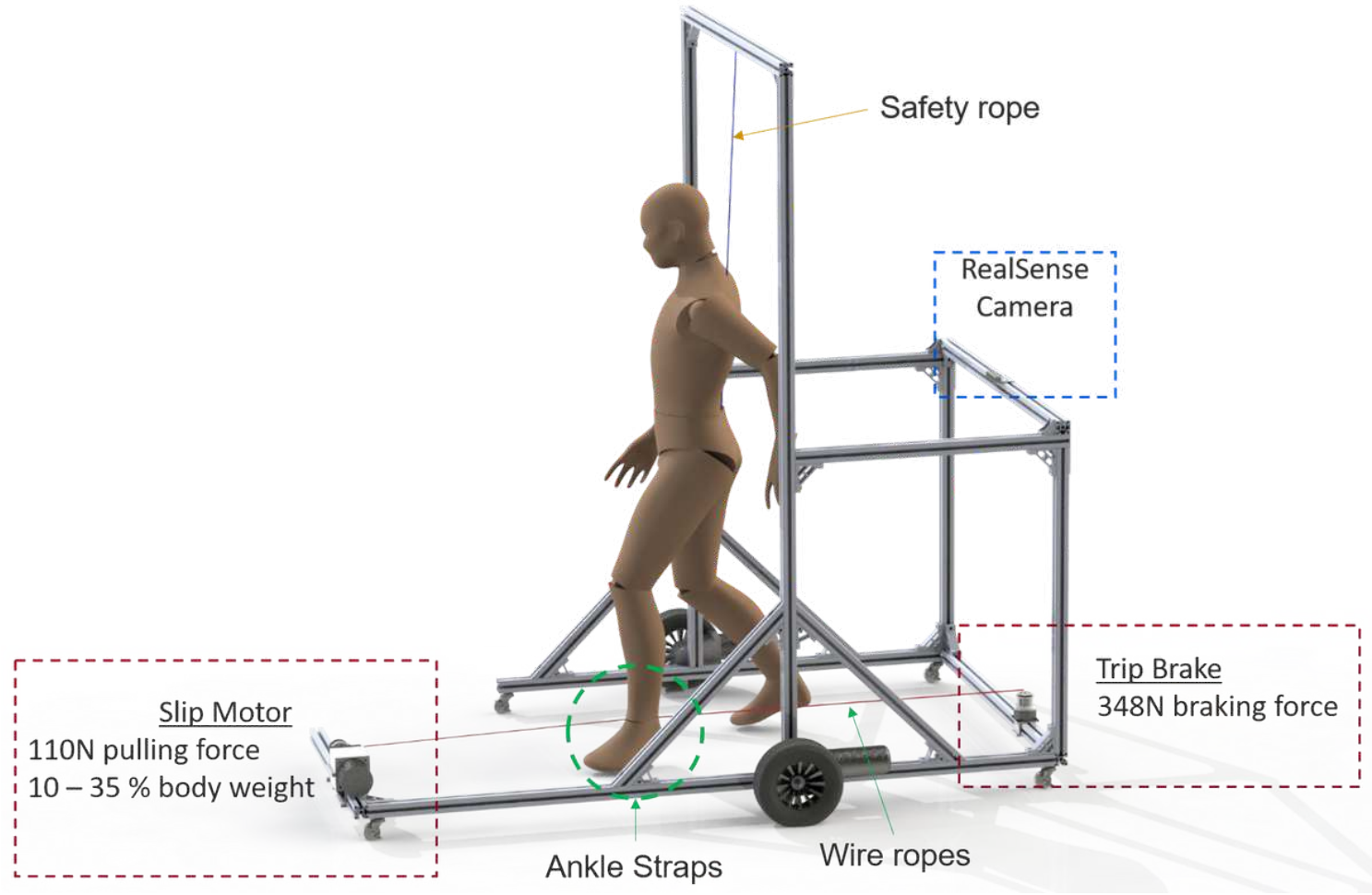

Figure 1

Fall inducing movable platform (FIMP). The structure was made from 40cm X 40cm aluminium profiles. A brake was used for trips induction and DC motor for slips. Slips and trips were induced on the left leg via wire rope (green dotted circle). A RealSense camera mounted at the back of the platform allowed for subject following technology. The safety rope mounted across the top of the platform prevented fall impact while having zero inertia on the subject during walking.

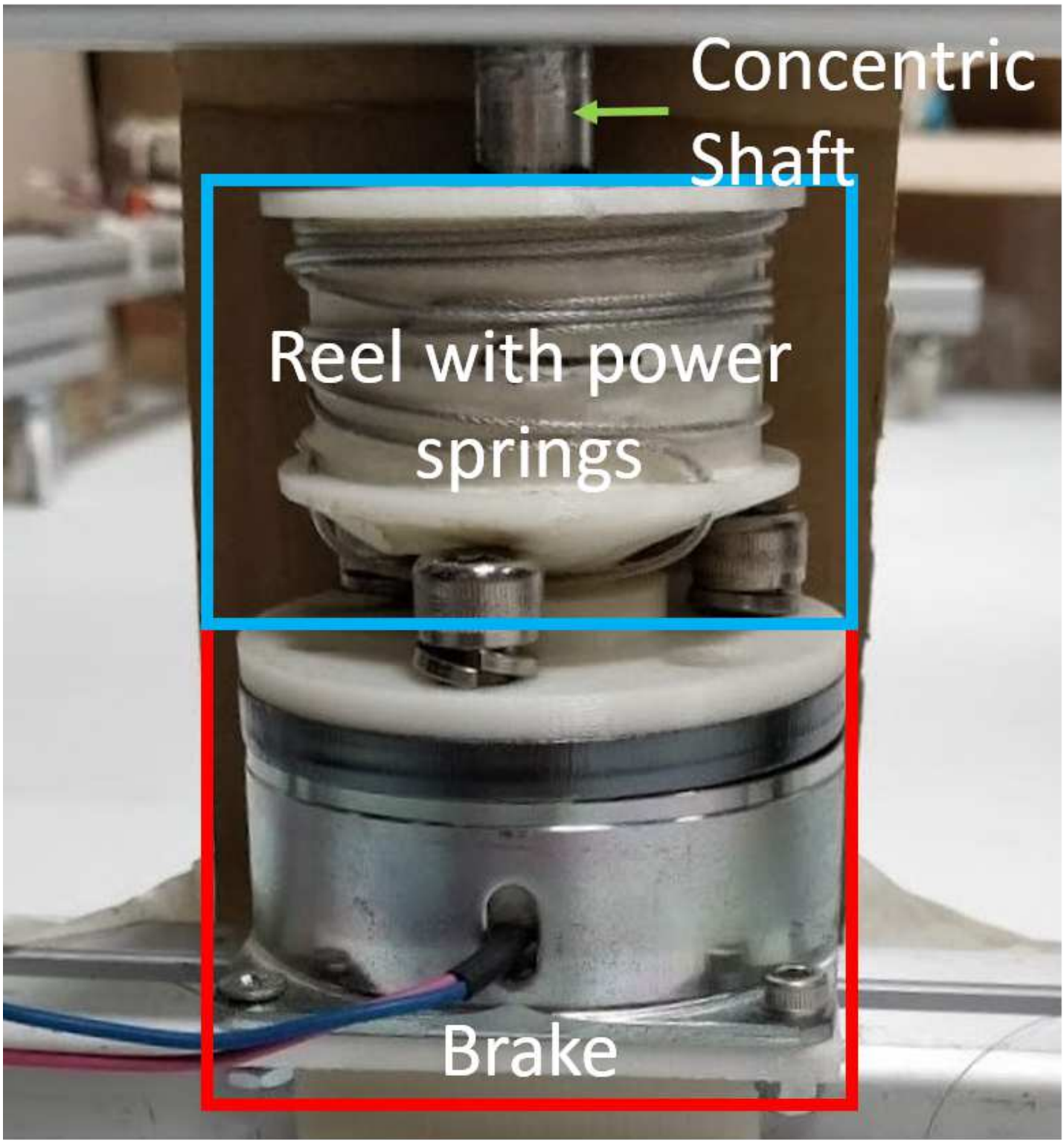

Figure 2

The trip brake mounted on FIMP with a concentric shaft keeping the reel with constant force spring centred.

Figure 3

The slip motor was mounted horizontally with its output shaft connected to a bi-directional clutch and finally to a constant force spring. To prevent over-reeling of the motor, a thick acrylic sheet with a hole prevented the cable endings from being reeled in. The hole also guided the wire rope into the reel getting tangled. A fuse was added in series with the motor to prevent excessive torque.

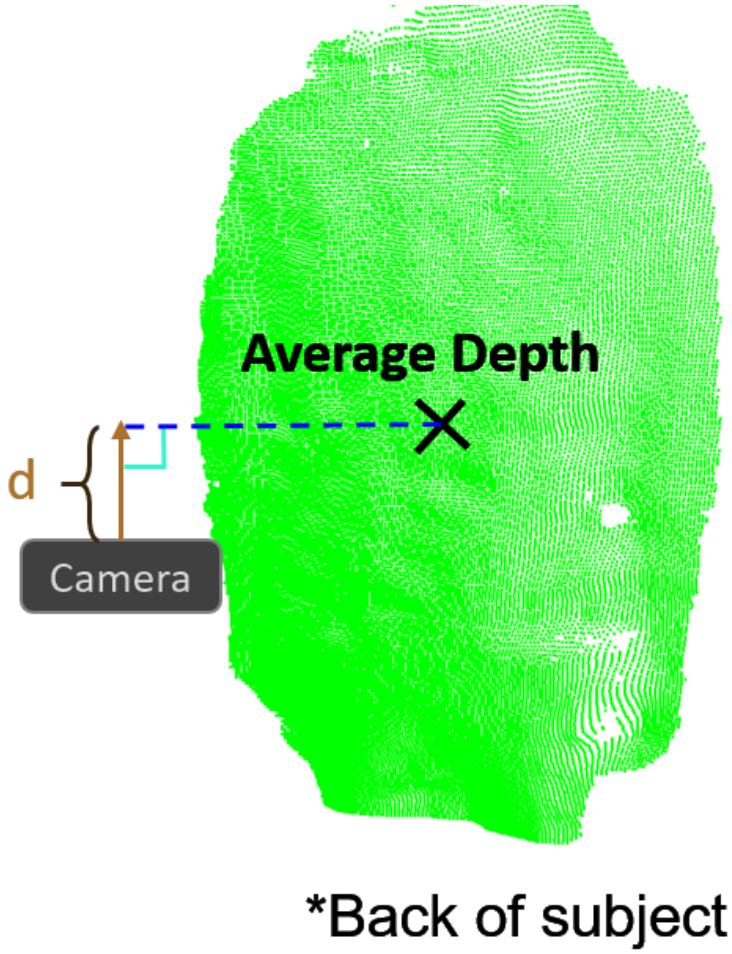

Figure 4

Calculation of forward distance for the subject follower algorithm.

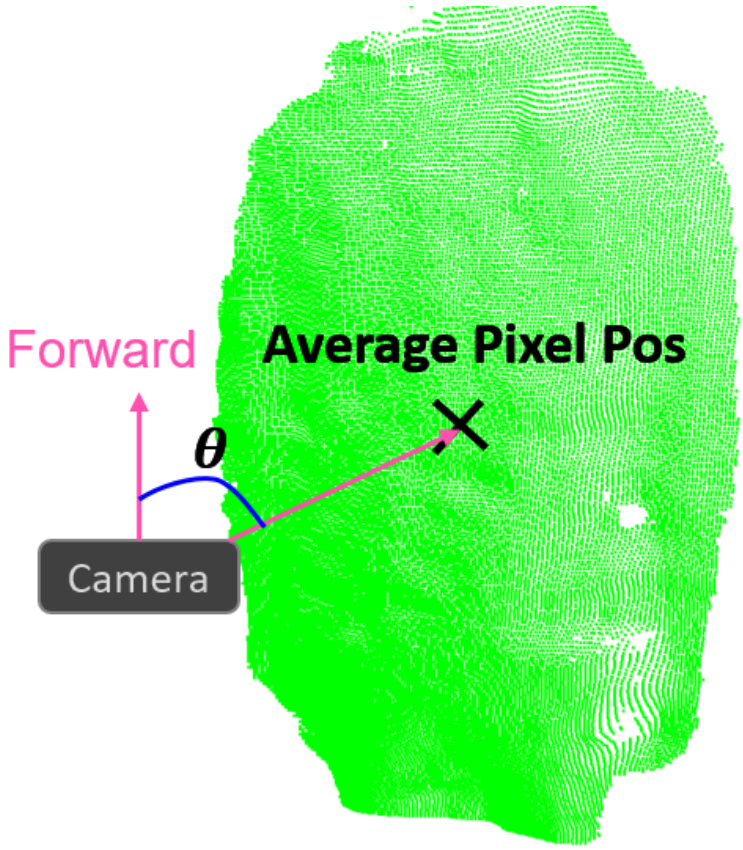

Figure 5

Calculation of orientation angle for the subject follower algorithm.

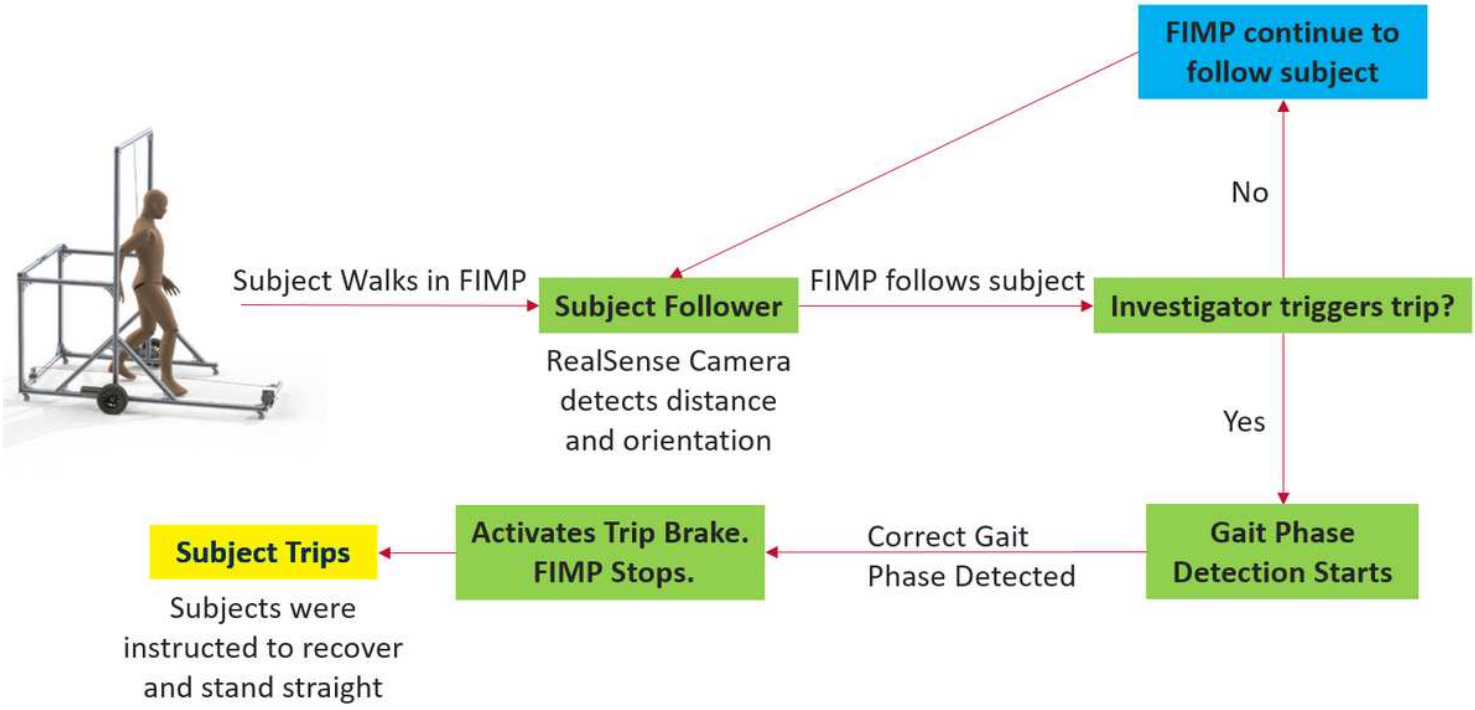

Figure 6

System control of FIMP. Subject starts walking in FIMP. RealSense camera detects the user's position and drives the wheels to follow the subject. As FIMP follows, it polls for investigator trigger via a button pressed for intention to trip the subject. When the button is pressed, the system automatically initiates the gait phase detection algorithm. Upon the correctly detected gait phase, the system immediately stops the wheels of FIMP and activates the trip brake. Subjects are instructed to recover and stand straight after the trip.

Figure 7

All subjects started by wearing a base Velcro suit, then a torso and seat safety harness and finally the Velcro belt with all the gait phase detection hardware. IMUs were placed on the torso, thighs and shanks of the subject, although only the left thigh and torso's IMU were used. Finally, reflective markers were secured onto the subject via the Velcro suit.

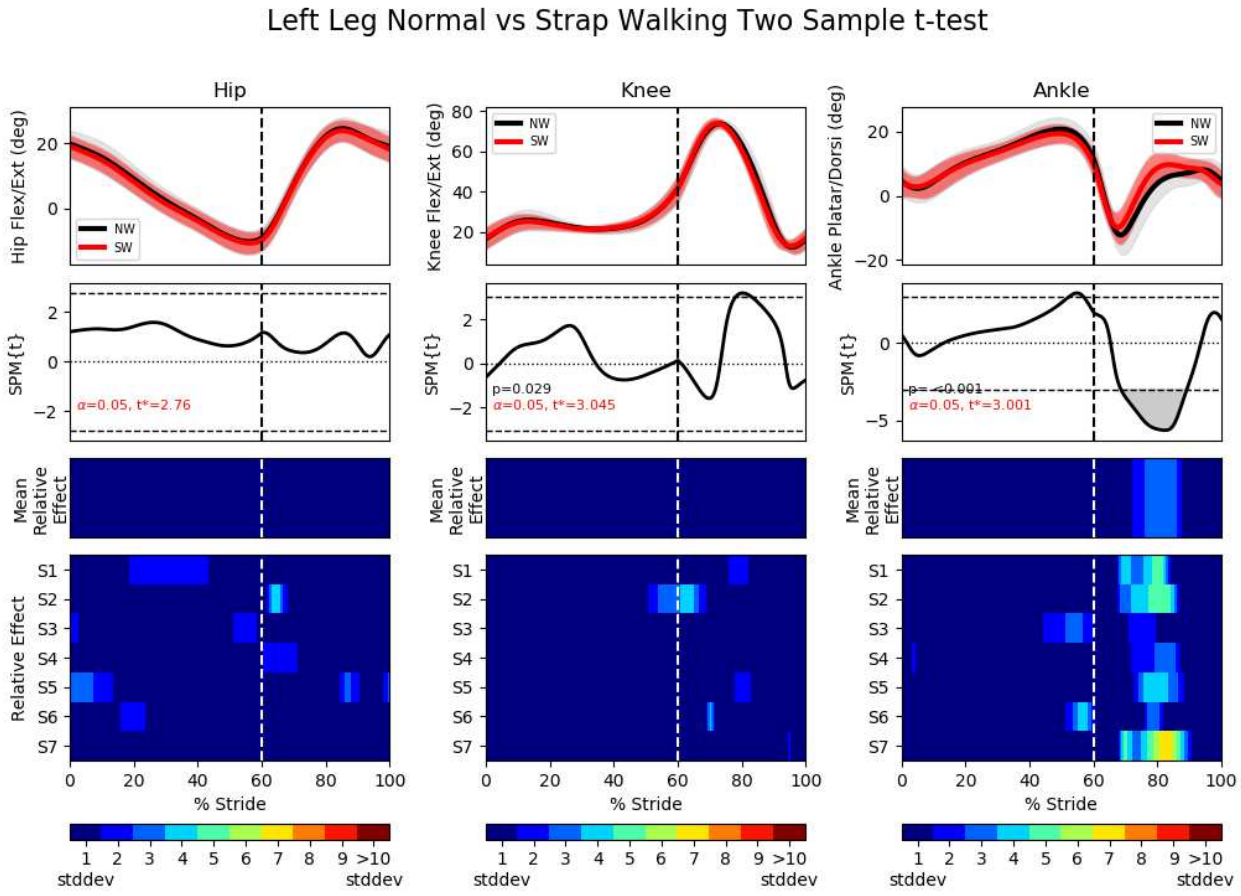

Figure 8

Comparison of NormalWalking (NW) vs StrapWalking (SW) trials for the left leg using SPM1D. The left leg is the leg with the ankle strap attached for fall induction. Top row indicates the mean hip, knee and ankle exion angles for all subjects and standard deviation clouds; mean (± st.dev). Second row indicates the Two-sample t-test on the data in top row. The third and last rows show a colour map highlighting the t-test significant differences for the all subjects' combined and their individual NW vs SW trials. Significant differences are seen in the ankle joint during the mid-swing phase for the majority of the subjects. There are also differences found in the knee during the mid-swing phase, but it is less consistent among all the subjects.

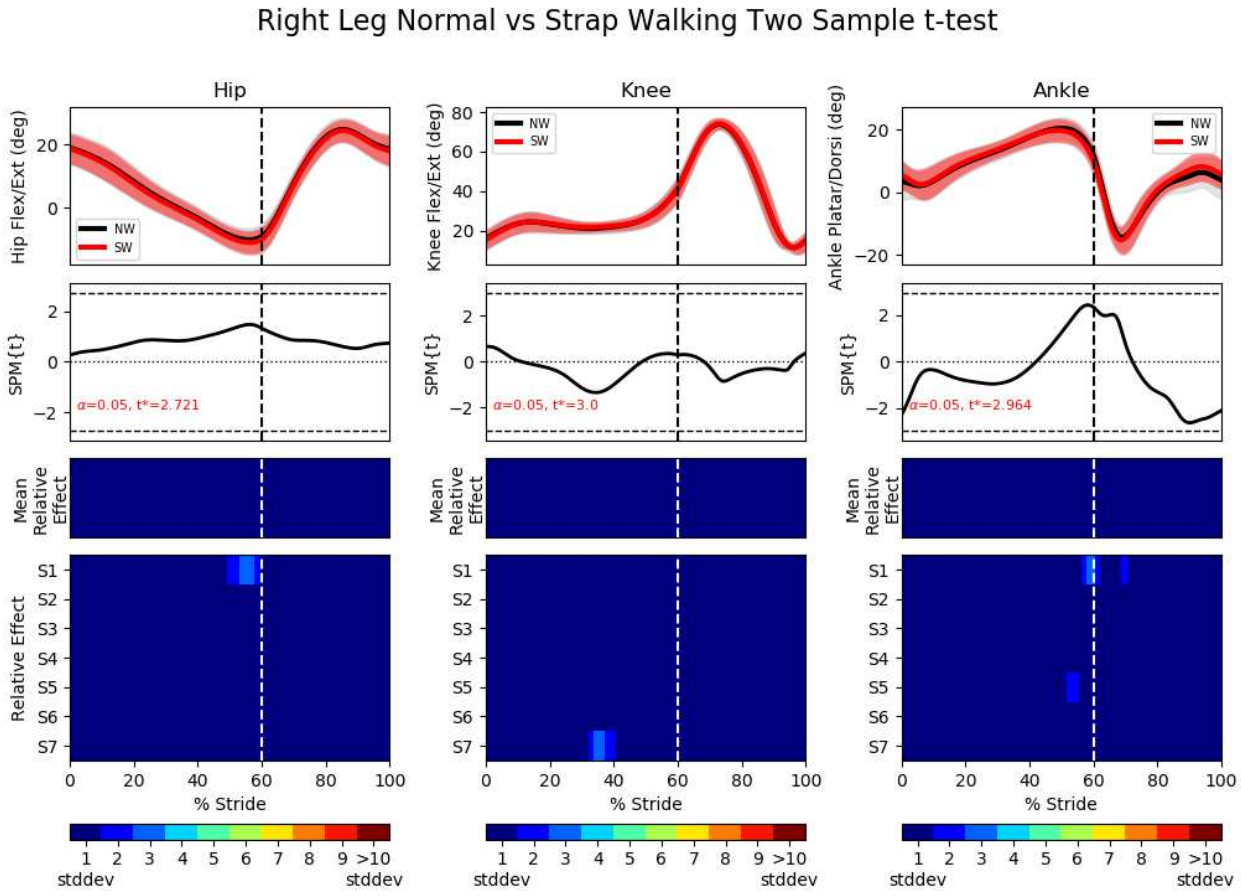

Figure 9

Comparison of NormalWalking (NW) vs StrapWalking (SW) trials for the right leg using SPM1D. The right leg is not attached to any ankle straps. Top row indicates the mean hip, knee and ankle exion angles for all subjects and standard deviation clouds; mean (± st.dev). The third and last rows show a colour map highlighting the t-test significant differences for the all subjects' combined and their individual NW vs SW trials. The last row shows the significant different effect size of individuals. No significant differences are found in any of the joints for the majority of the subjects

Figure 10

End-swing fall sequence (left to right) induced by the brake attached to the subject's ankle via a wire.

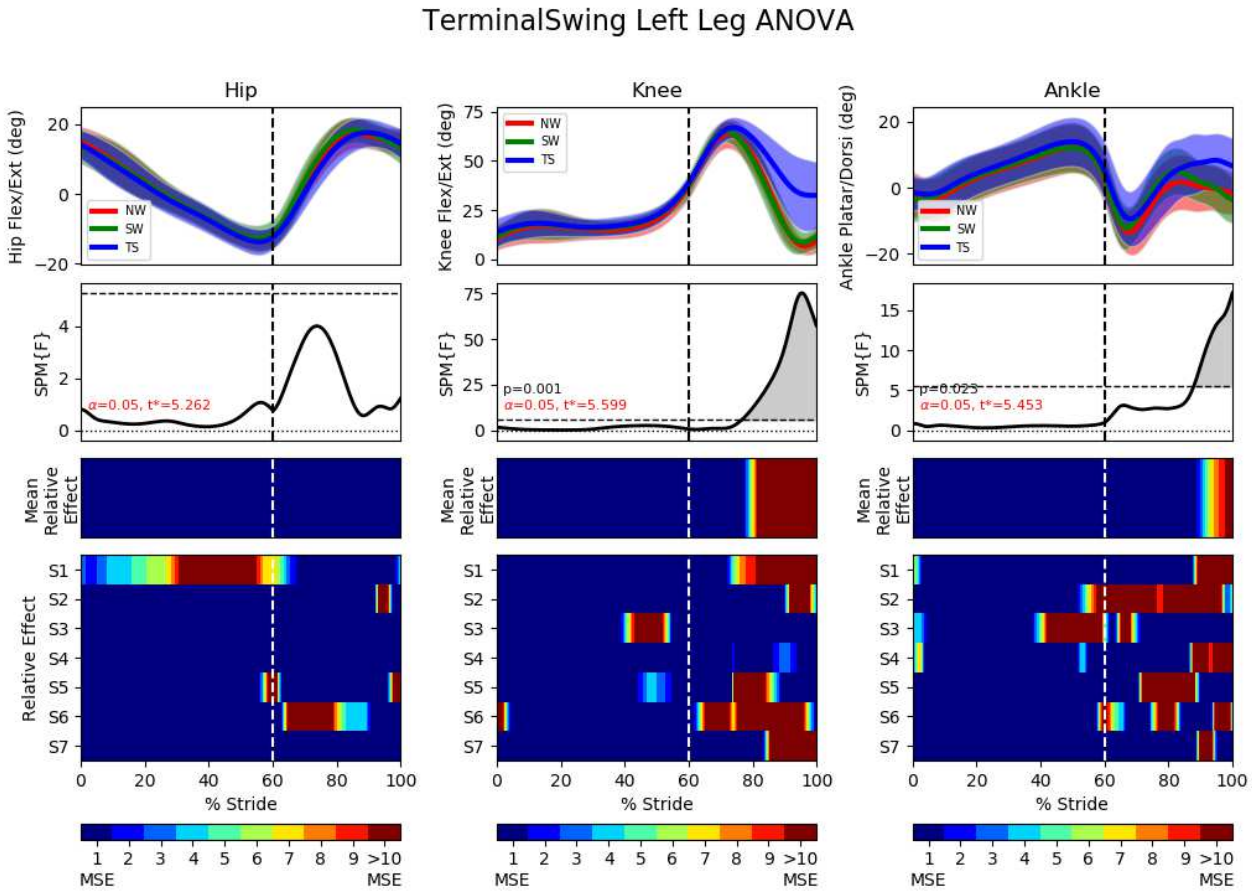

Figure 11

One-way repeated measure ANOVA comparison of NormalWalking (NW) vs StrapWalking (SW) vs TerminalSwing (TS) trials for the left leg with SPM1D. The left leg is attached to the ankle straps with a brake at the opposite end. Top row indicates the mean hip, knee and ankle exion angles for all subjects and standard deviation clouds; mean (± st.dev). Second row indicates the ANOVA test on the data shown in top row. Third row shows a colour map highlighting significant differences of the ANOVA result in

second row. The last row shows the significant different effect size of individuals. Significant differences are observed in the knee and ankle joints near the terminal-swing phase.

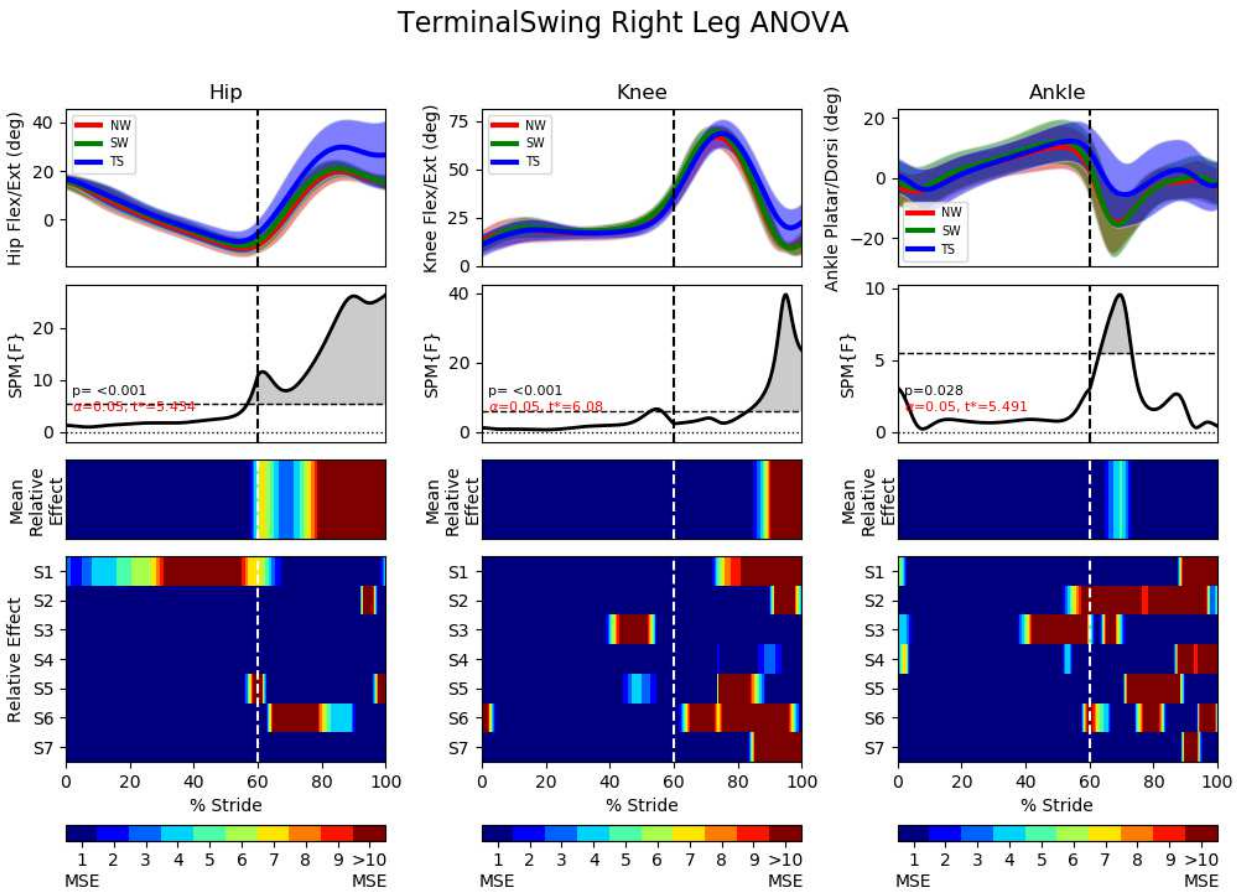

Figure 12

One-way repeated measure ANOVA comparison of NormalWalking (NW) vs StrapWalking (SW) vs TerminalSwing (TS) trials for the right leg with SPM1D. The right leg is attached not attached to any ankle straps. Top row indicates the mean hip, knee and ankle exion angles for all subjects and standard deviation clouds; mean (± st.dev). Second row indicates the ANOVA test on the data shown in top row. Third row shows a colour map highlighting significant differences of the ANOVA result in second row. The last row shows the significant different effect size of individuals. The hip joints have the most pronounced differences when comparing to NW and SW. The knee joint experiences lower extension angle at the terminal-swing phase, while the ankle joint has lower plantar exion at the early swing phase.

Figure 13

Mid-swing fall sequence (left to right) induced by the brake attached to the subject's ankle via a wire.

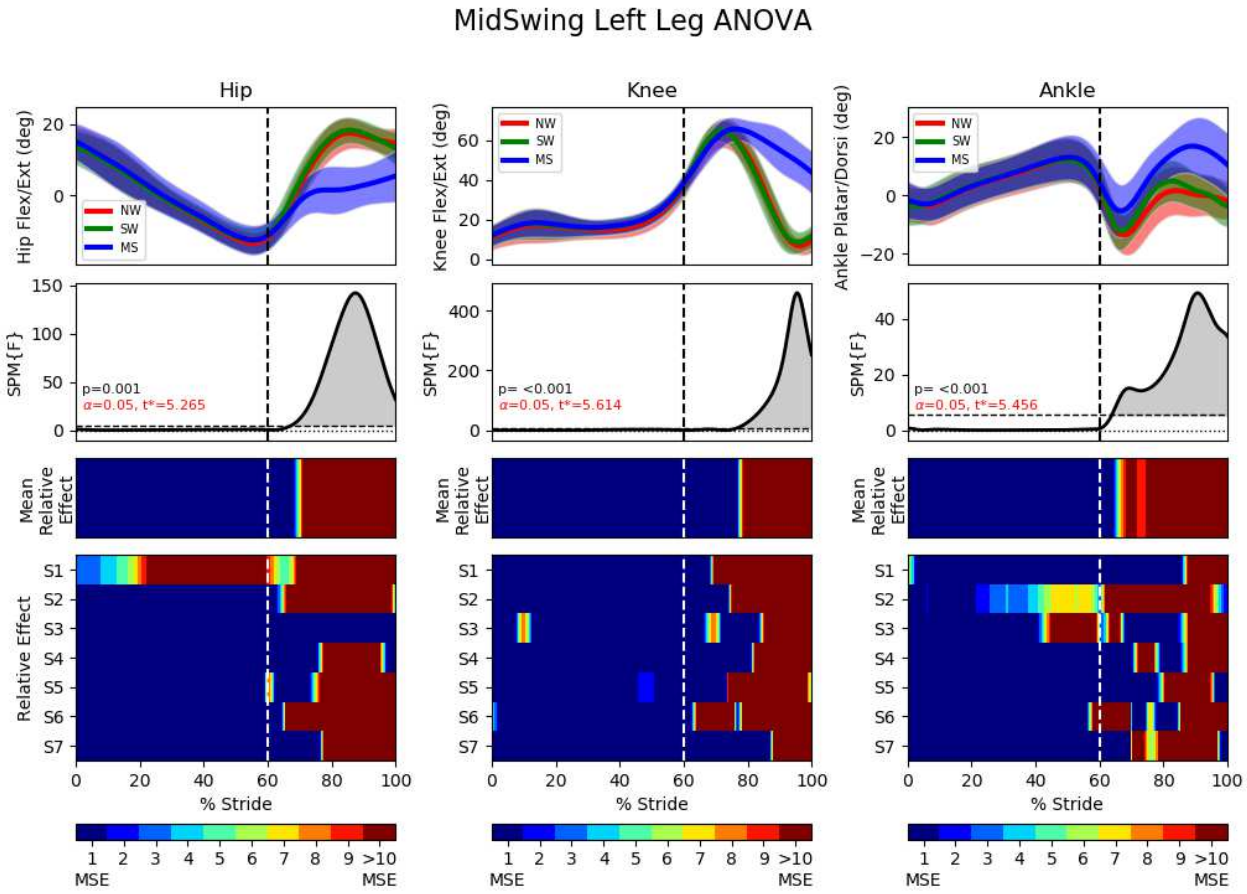

Figure 14

One-way repeated measure ANOVA comparison of NormalWalking (NW) vs StrapWalking (SW) vs MidSwing (MS) trials for the left leg with SPM1D. The left leg is attached to the ankle straps with a brake at the opposite end. Top row indicates the mean hip, knee and ankle exion angles for all subjects and standard deviation clouds; mean (± st.dev). Second row indicates the ANOVA test on the data shown in top row. Third row shows a colour map highlighting significant differences of the ANOVA result in second

row. The last row shows the significant different effect size of individuals. Significant differences are observed in the knee and ankle joints near the terminal-swing phase.

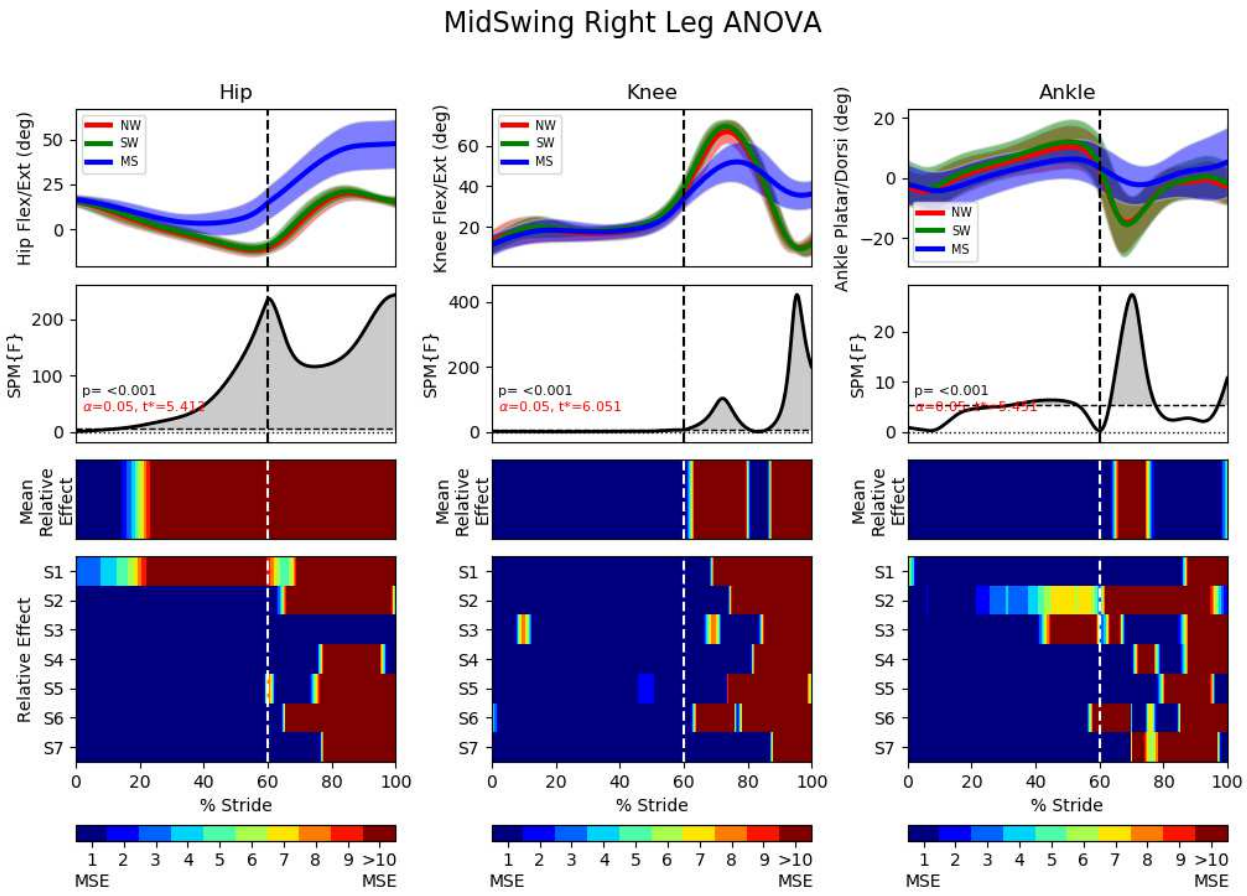

Figure 15

One-way repeated measure ANOVA comparison of NormalWalking (NW) vs StrapWalking (SW) vs MidSwing (MS) trials for the right leg with SPM1D. The right leg is not attached to any ankle straps. Top row indicates the mean hip, knee and ankle exion angles for all subjects and standard deviation clouds; mean (± st.dev). Second row indicates the ANOVA test on the data shown in top row. Third row shows a colour map highlighting significant differences of the ANOVA result in second row. The last row shows the significant different effect size of individuals. Significant differences are observed in the knee and ankle joints near the terminal-swing phase.

Figure 16

Slip fall sequence (left to right) induced by the motor attached to the subject's ankle via a wire. A low friction sliding sheet was placed on the ground to reduce foot to ground friction.

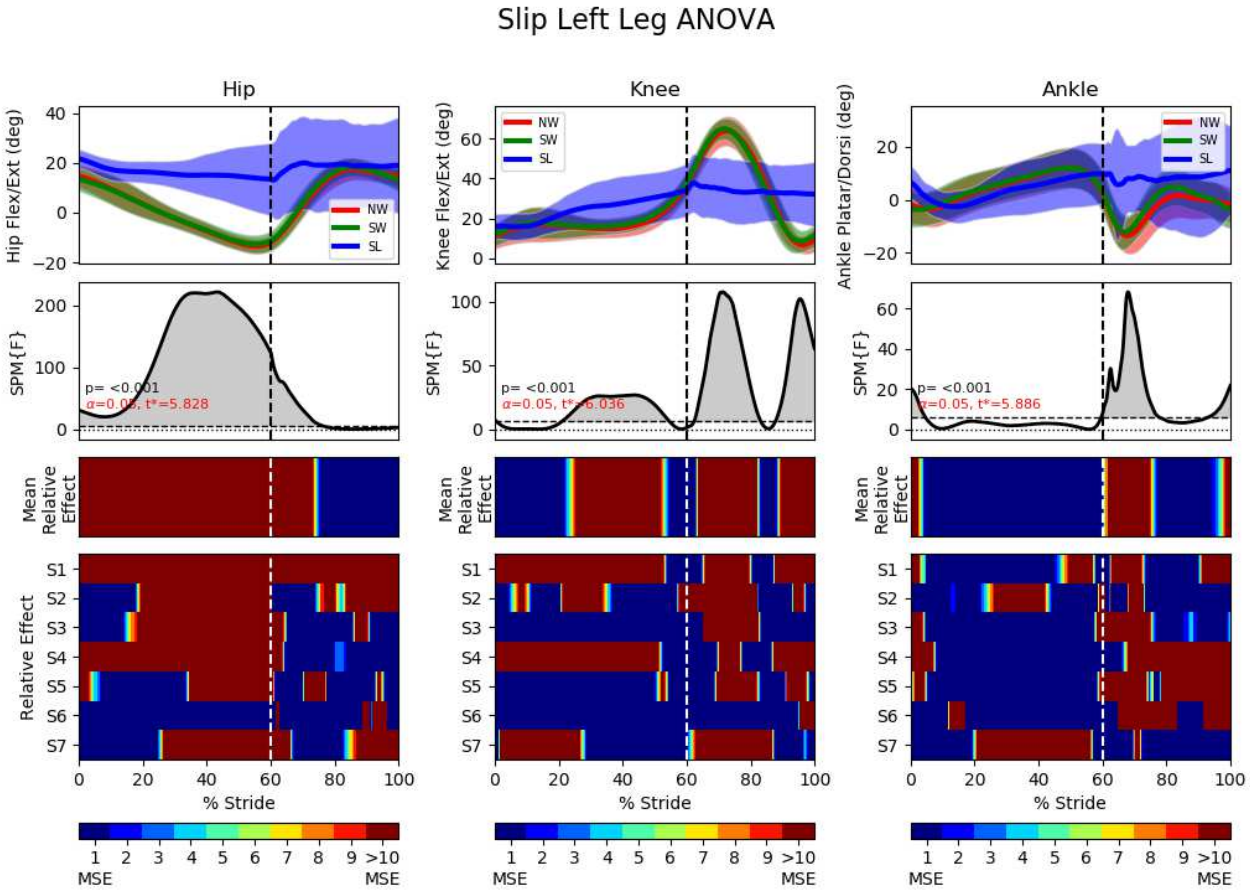

Figure 17

One-way repeated measure ANOVA comparison of NormalWalking (NW) vs StrapWalking (SW) vs Slip (SL) trials for the left leg with SPM1D. The left leg is attached to the ankle straps with a brake at the opposite end. Top row indicates the mean hip, knee and ankle exion angles for all subjects and standard deviation clouds; mean (± st.dev). Second row indicates the ANOVA test on the data shown in top row. Third row shows a colour map highlighting significant differences of the ANOVA result in second row. The last row shows the significant different effect size of individuals. All the joint angles are relatively constant as compared to NormalWalking. This indicates that stiffening of joints occur during slips.

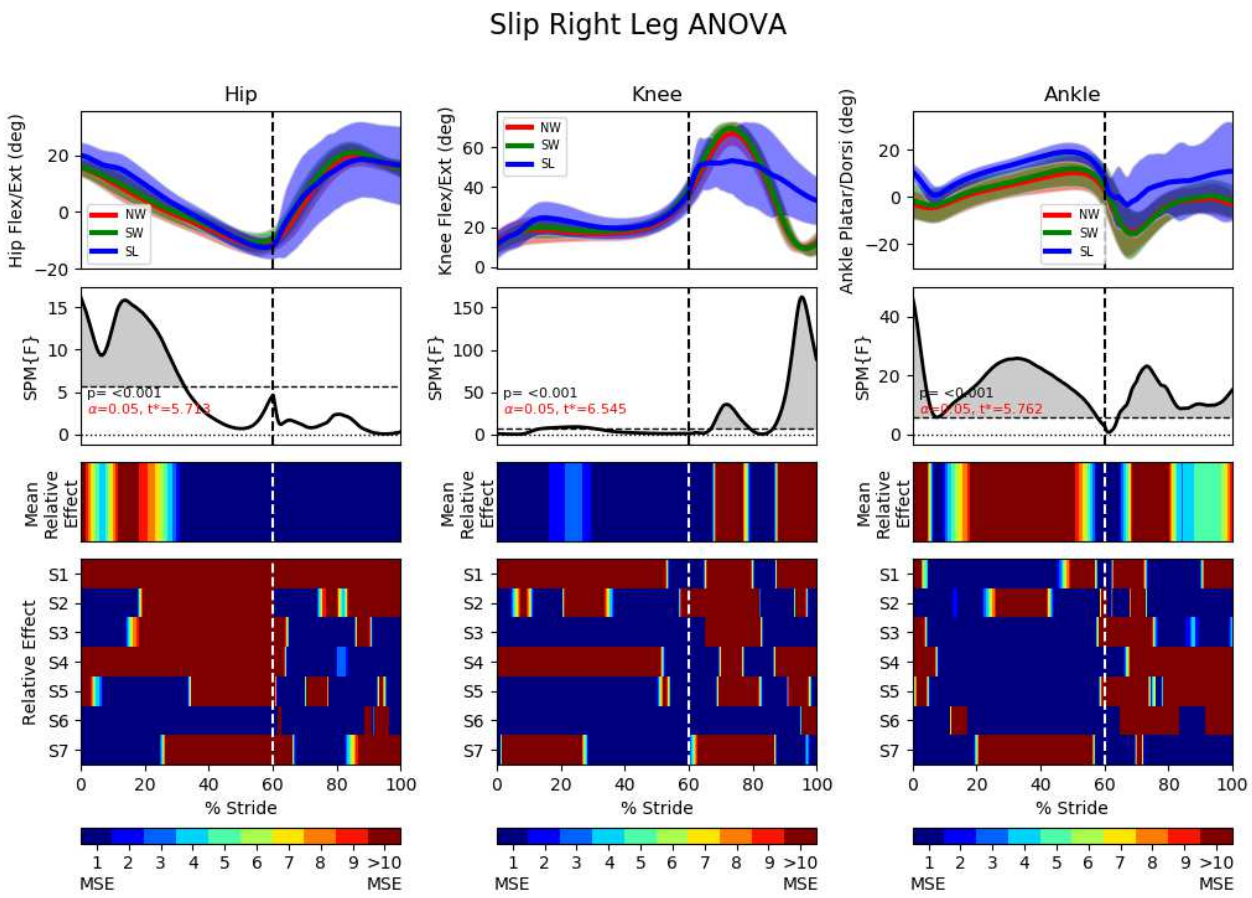

Figure 18

One-way repeated measure ANOVA comparison of NormalWalking (NW) vs StrapWalking (SW) vs Slip (SL) trials for the right leg with SPM1D. The right leg is not attached to any ankle straps. Top row indicates the mean hip, knee and ankle exion angles for all subjects and standard deviation clouds; mean (± st.dev). Second row indicates the ANOVA test on the data shown in top row. Third row shows a colour map highlighting significant differences of the ANOVA result in second row. The last row shows the significant different effect size of individuals. The right knee and ankle has a more constant joint angle throughout the swing phase, indicating the adoption of the surfing strategy (keeping foot at and close to ground).

Supplementary Files

This is a list of supplementary files associated with this preprint. Click to download.

- Additionalfile2.pdf
- Additionalfile1.mp4